

Instituto Tecnológico y de Estudios Superiores de Occidente

Reconocimiento de validez oficial de estudios de nivel superior según acuerdo secretarial 15018, publicado en el Diario Oficial de la Federación del 29 de noviembre de 1976.

Departamento de Electrónica, Sistemas e Informática
Maestría en Diseño Electrónico



REPORTE DE FORMACIÓN COMPLEMENTARIA EN ÁREA DE CONCENTRACIÓN EN DISEÑO ELECTRÓNICO DE ALTA FRECUENCIA

TRABAJO RECEPCIONAL que para obtener el **GRADO** de
MAESTRO EN DISEÑO ELECTRÓNICO

Presenta: **JOSÉ ANTONIO RODRÍGUEZ CASTAÑEDA**

Asesor: **OMAR HUMBERTO LONGORIA GANDARA**

Tlaquepaque, Jalisco. Octubre de 2020.

Content

Introduction	1
1. Band-Stop Filter	3
1.1. INTRODUCTION	3
1.2. BACKGROUND	3
1.3. RESULTS	4
1.4. CONCLUSIONS	5
2. Monte Carlo Analysis of an Active Clamping Circuit in a Low Side Driver Power Output	6
2.1. INTRODUCTION	6
2.2. BACKGROUND	6
2.3. RESULTS	7
2.4. CONCLUSIONS	8
3. Power Dissipation During On Time Optimization of an Active Clamping Circuit in a Low Side Driver Power Output	9
3.1. INTRODUCTION	9
3.2. BACKGROUND	9
3.3. RESULTS	12
3.4. CONCLUSIONS	13
4. Conclusions	15
Appendix	17
A. FINAL PROJECT – BAND STOP FILTER	19
B. MONTECARLO ANALYSIS OF AN ACTIVE CLAMPING CIRCUIT IN A LOW SIDE DRIVER POWER OUTPUT	43
C. ON TIME AND POWER OPTIMIZATION OF AN ACTIVE CLAMPING CIRCUIT IN A LOW SIDE DRIVER POWER OUTPUT	64
D. REFERENCES	85

Introduction

Automotive engine electronic controllers are becoming more and more complex due to stricter vehicle gas emission standards around the world. The Engine Controller Unit (ECU) helps increase fuel consumption efficiency by monitoring and controlling multiple valves, sensors, and actuators [1]. The fuel pump, the engine starter, or injection solenoids are common examples of valves and actuators. The engine of the vehicle is controlled by the ECU, following the driver's instructions and considering several rules to reach a trade-off between performance and the control of gas emissions.

In addition, the ECU requires a smaller packaging for the housing of the electronic controller that leads to a higher power density. This will result in more heat dissipation by the ECU housing; therefore, the engineering team has to carefully design the power dissipation of every single module inside the ECU. Consequently, thermal management of the ECU housing has become a challenge in the automotive industry [2]. Power dissipation optimization of the electronic components, for instance, is one of the approaches developed on the *Modeling and Circuit Design based on Optimization* subject of this specialization, trying to reduce the heat produced by the switching components in the ECU.

The present document consists of a summary of the final projects accomplished over High Frequency Electronic Design concentration area. The concentration area is based on three subjects: *High Frequency Electronic Design, Electronic Circuit Simulation Methods, and Modeling and Circuit Design based on Optimization*. The aim of study of these subjects is to implement an optimization algorithm to determine the components of the Low Side Driver circuit with active clamping that satisfy the discharge time requirements with the minimum power dissipation.

Analysis and design of high-frequency electronic circuits, CAD tools for electronic devices and circuit simulation, and advanced numerical optimization techniques to modeling and design were competences provided by the selected concentration area that contributed to the development of the investigation subject.

1. Band-Stop Filter

1.1. Introduction

Final project of the *High Frequency Electronic Design* subject. The function of a Microstrip band-stop filter is to attenuate an undesired band of frequencies while to allow to pass the others using Microstrip lines with a specific geometry structure to create dielectric resonators. The objective of this project is to: design, implement and, evaluate the results of a Chebyshev third order band-stop filter with a central frequency of 3.4GHz and 5% of fractional bandwidth. In addition, the aim of this project is to applicate the knowledge of circuit and 3D planar electromagnetic simulators.

1.2. Background

The design of a Chebyshev filter is based on the elements of the low-pass prototype of third order to obtain the normalized reactance using equation (1-2-1).

$$x_i = w_0 L_i = \frac{1}{w_0 C_i} = Z_0 \left(\frac{Z_U}{Z_0} \right)^2 \frac{g_0}{g_i \Omega_c FBW} \quad \text{for } i = 0 \text{ to } n \quad (1-2-1)$$

The design procedure is based on the creation of “L” resonators coupled to a main Microstrip line with a length half of the electrical length λ and separated from the transmission line with appropriate “S” length. A parameter sweep simulation is used to obtain the proper “S” value in relation to each “Xx/Z0” reactance calculated with (1-2-1) using the parameter extraction described on Figure 1-2-1 using single resonators.

Finally, the complete structure is assembled with all the “L” resonators coupled to the main Microstrip transmission line. An example of five resonators band-stop filter is shown on Figure 1-2-2.

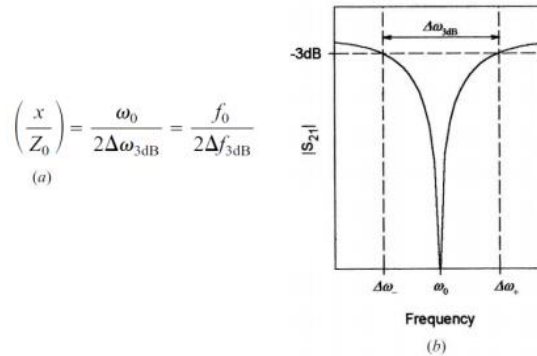


Figure 1-2-1. (a) Formula to correlate x/Z_0 and the frequency response of the simulator. (b) Frequency response measurement. [3]

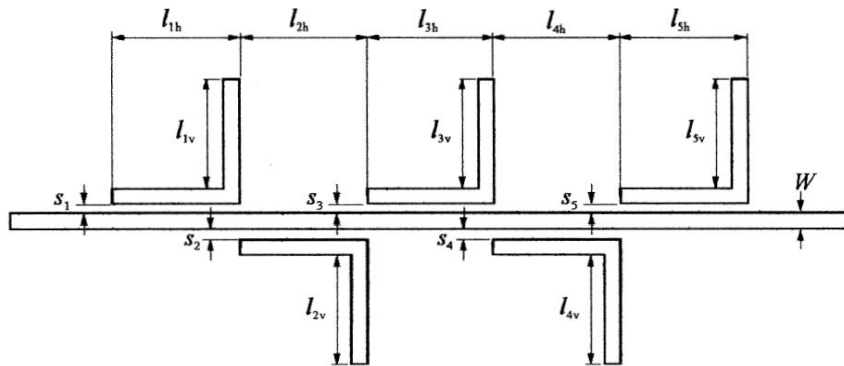


Figure 1-2-2. (a) Band-stop filter of fifth order using "L" resonators. [3]

1.3. Results

As a result of multiple parameter sweeps for the separation length "S" in the two "L" resonator prototypes using a circuitual simulator, as well as a 3D planar electromagnetic simulator, the proper "Xx/Z0" reactance were matched to the calculation results. The third order Chebyshev filter layout with the integration of the three resonators in the 3D planar electromagnetic simulator is shown on Figure 1-3-1. The central frequency of the simulator result is 3.403GHz, marked as "m3" at the bottom of the Figure 1-3-2. Finally, the markers "m1" and "m2" states the Fractional Bandwidth of the filter with 3.317GHz and 3.484GHz.

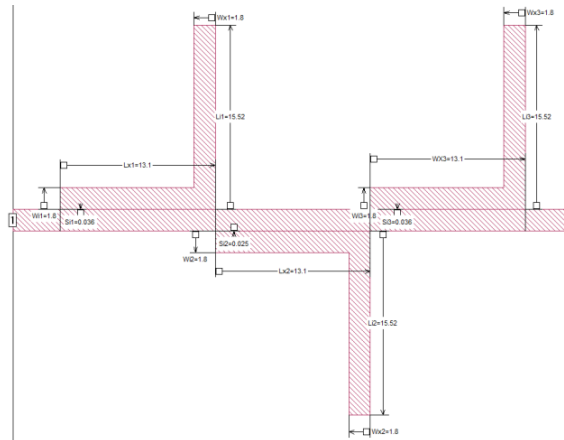


Figure 1-3-1. Third order Chebyshev stop-band filter layout.

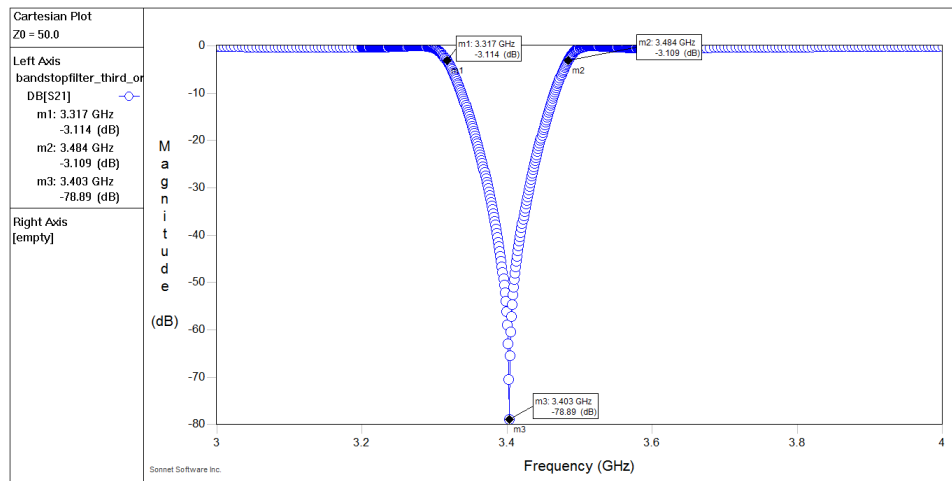


Figure 1-3-2. Third order Chebyshev stop-band filter frequency response.

1.4. Conclusions

The Band-stop filter development using Microstrip line technology project provided the crucial skills about design, construction and functionality of resonant filters using coupled transmission lines. On top of that, the skills for configuring and using electromagnetic simulators were also deployed during this project. Finally, it is wanted to highlight the importance of understand and consider the differences between the calculation, the electric simulator and, the 3D planar electromagnetic simulator results due to the intrinsic characteristics of evaluation of each method.

2. Monte Carlo Analysis of an Active Clamping Circuit in a Low Side Driver Power Output

2.1. Introduction

Final project of the *Electronic Circuit Simulation Methods* subject. Power outputs are used in automotive electronics industry in order to control valves such as the Fuel Pump or the Starter of the Engine. This type of actuators, which can be represented as a resistance in series with an inductor, are driven commonly by a circuit named Low Side Driver (LSD). The aim of this project is to perform a Monte Carlo Analysis (MCA) over an Active Clamping Circuit, used on a Low Side Driver Power Out to accelerate the current decay of an inductive-resistive valve, in order to evaluate the behavior of the clamping voltage taking in consideration the components tolerance and ambient temperature variation. The MCA will be performed using MATLAB® together with a SPICE engine to perform the electrical simulations.

2.2. Background

For analysis and simulation purposes, automotive actuators for controlling valves can have a simple electrical representation using a resistor in series with an inductor. The inductor stores energy in form of a magnetic field when a current is flowing through its terminals. The magnetic field will be stronger as the current that passes through the inductor increases as well as the energy stored. In addition, the inductor has a tendency to resist changes in the current as a result of its ability to store energy, producing a voltage change over the terminals in the opposite direction of the current polarity.

The purpose of the LSD circuit is to work as a ground path enabler for specific loads that are connected to the car's battery. In addition, the LSD active clamping circuitry is designed to handle the energy stored on the inductor when the ground path is not enabled. The active clamping circuit accelerate the discharge of the stored energy on the inductor using the main MOSFET in ohmic region and increasing the voltage of the output pin. Figure 2-2-1 illustrates the LSD with active clamping circuit.

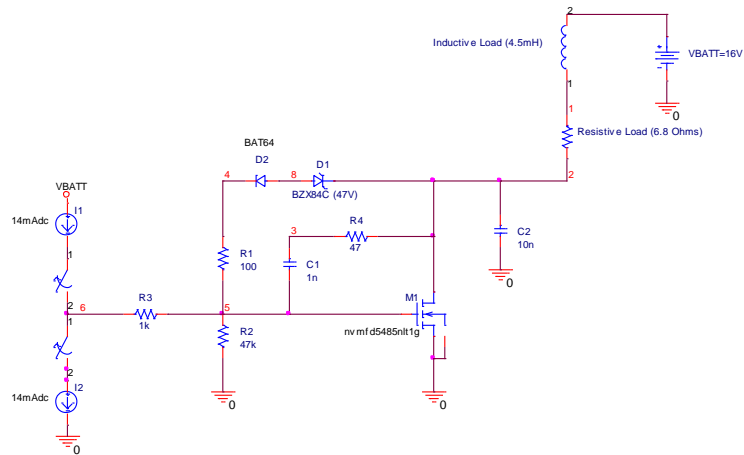


Figure 2-2-1. Representation of a Low Side Driver circuit with active clamping and pre-driver ASIC..

2.3. Results

The active clamping circuit is simulated using the text mode circuit simulator WINSPIICE®. For this project, WINSPIICE® will be executing scripts with the active clamping circuit description generated by the third-party program: MATLAB®. The third-party program is in charge of the execution of the MCA of the circuit with the following task: calculate circuit specific run parameters, execute WINSPIICE® with the current circuit, save the transient response, calculate the active clamping average voltage and present the result the MCA over “N” number of outcomes.

Component	Value	Tolerance
R1	100 Ω	5%
R2	4700 Ω	1%
R3	1000 Ω	1%
R4	47 Ω	1%
C1	1nF	5%
C2	10nF	5%
Vb	47V*	2%
RL	6.8 Ω	1%
LL	4.5mH	5%
Temp	25°C	-40°C and 105°C

Table 2-2-1. Value and tolerance per component for MCA calculation.

The components and temperature of the LSD circuit MCA are assorted using the tolerances shown on Table 2-2-1 and following a Gaussian distribution. The limits used for the yield calculation of the active clamping are defined by a Worst-Case Analysis (WCA).

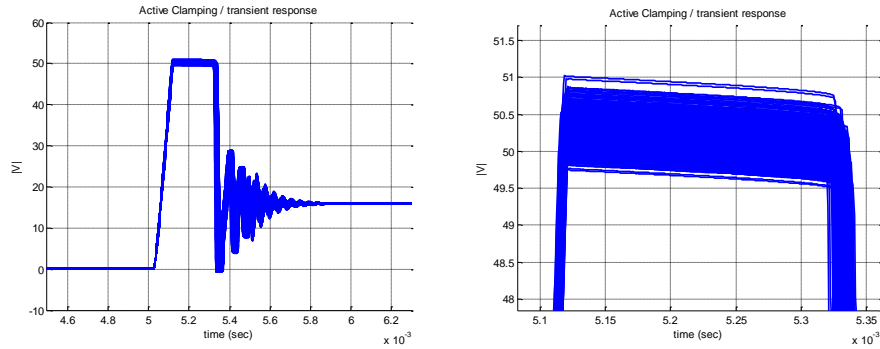


Figure 2-2-2. MCA results for the Active Clamping voltage [left] and zoom over active clamping zone [right] with a $N=500$ outcomes.

The Monte Carlo Analysis results for the active clamping voltage are shown on Figure 2-2-2. Besides the transient response and plotting, Yield and Histogram is presented to evaluate the limits provided by the WCA as shown on Figure 2-2-3.

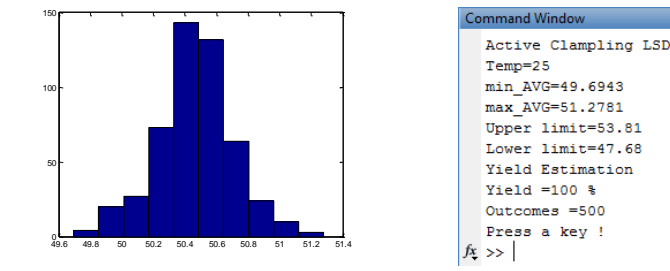


Figure 2-2-3. Histogram for the 500 outcomes for the MCA in the active clamping voltage.

2.4. Conclusions

The Monte Carlo Analysis over the LSD active clamping circuit endorsed that the limits provided by the WCA are correct considering a vast variation in the component's tolerance and ambient temperature. The WCA limits are done using extreme values for tolerances of the components without taking in consideration all the possible combinations that could lead to a “worst case”. The integration of WINSPICE® into the MATLAB® environment provided the enough flexibility to develop the MCA and present the statistical results on an automatized environment.

3. Power Dissipation During On Time Optimization of an Active Clamping Circuit in a Low Side Driver Power Output

3.1. Introduction

Final project of the *Modeling and Circuit Design based on Optimization* subject. Automotive engine electronic controllers are becoming more and more complex due to stricter vehicle gas emission standards around the world. The Engine Controller Unit (ECU) requires a smaller packaging for the housing of the electronic controller that leads to a higher power density. This will result in more heat dissipation by the ECU housing; therefore, the engineering team has to carefully design the power dissipation of every single module inside the ECU. Consequently, thermal management of the ECU housing has become a challenge in the automotive industry.

The intention of this project is to implement an optimization algorithm to find the components of the LSD circuit that satisfy the discharge time requirements having the minimum power dissipation. The optimization algorithm will be based on a “Minimax” formulation with box constraints. The purpose of the Minimax formulations is to reduce to a minimum the error of a model, in this case, a delimited circuit response with specific operation restrictions.

3.2. Background

For analysis and simulation purposes, automotive actuators for controlling valves can have a simple electrical representation using a resistor in series with an inductor. The inductor stores energy in form of a magnetic field when a current is flowing through its terminals. The purpose of the LSD circuit is to work as a ground path enabler for specific loads that are connected to the car’s battery. In addition, the LSD active clamping circuitry is designed to handle the energy stored on the inductor when the ground path is not enabled. Figure 3-2-1 illustrates the LSD with active clamping circuit.

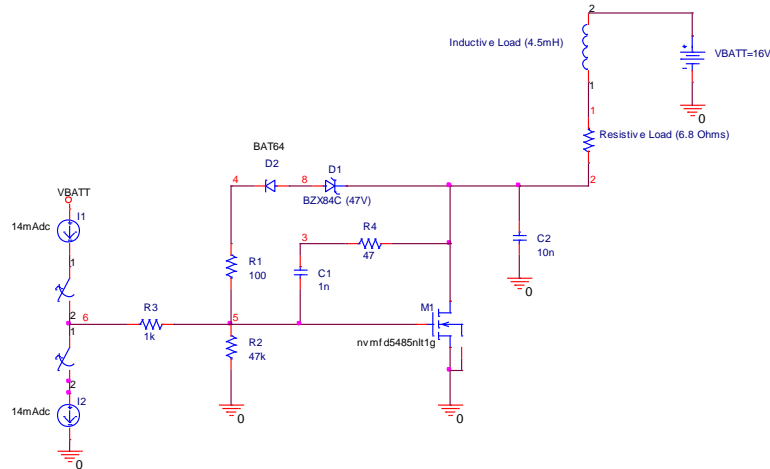


Figure 3-2-1. Representation of a Low Side Driver circuit with active clamping and pre-driver ASIC..

The active clamping circuit will be simulated using the circuit simulator WINSPICE®. WINSPICE® is based on SPICE (*Simulation Program with Integrated Circuits Emphasis*), which is an international standard for nonlinear dc, nonlinear transient, and linear ac circuit analysis.

Moreover, MATLAB® will be used to implement the optimization algorithm to find the components of the LSD circuit with active clamping that satisfy the discharge time requirements with minimal power dissipation. The optimization algorithm requires an iterative process of the key parameter modifications in the circuit description, an evaluation of that circuit response on the simulator, and a target error calculation.

A communication channel between MATLAB® and WINSPICE® is necessary to perform the evaluation of the circuit response with the parameters calculated by the optimization algorithm. Therefore, a WINSPICE® driver for MATLAB® was implemented following the class notes from the graduate course “Simulation Methods for Electronic Circuits” by Dr. J. E. Rayas Sánchez. This driver allows MATLAB® to create simulation scripts and properly execute WINSPICE® to meet the optimization requirements.

The variables, which are subject of the optimization process, are the breakdown voltage of the D1 zener in volts (V), the resistor R4 value in ohms (Ω) and the value of the capacitor C1 expressed in nanofarads (nF). The vector of the optimization variables is $x = [V_b(V) R_4(\Omega) C_1(nF)]^T$ and with an starting point of $x_0 = [33 \ 47 \ 1]^T$. From circuit response at the optimization starting point, shown in Figure 3-2-2, the Power $P_{AC_{x_0}} = 12.1237mW$ and $OnTime_{AC_{x_0}} = 354us$ was calculated.

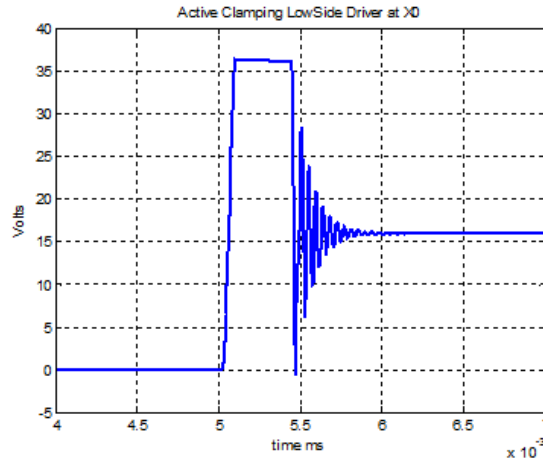


Figure 3-2-2. Active clamping circuit response at x_0 starting point.

The constraints or design limitations of the circuit behavior during the active discharge are the power dissipation and the OnTime, expressed as “ P_{AC} ” and “ OT_{AC} ” with a respective limits of $P_{AC} < 7.5mW = s_2^{UB}$ and $OT_{AC} < 150us = s_1^{UB}$.

The purpose of minimax formulations is to minimize the maximum error of a function in comparison with the specifications. The minimax formulation for the active clamping optimization problem can be represented with EQ 3-2-1 with a k-th error function expressed on EQ 3-2-2 with $\epsilon_1 = s_1^{UB}/100$ and $\epsilon_2 = s_2^{UB}/100$. The Manhattan norm was used for the error calculation.

$$x^* = arg \min_x \max\{... e_k(x) ... \} \quad (3-2-1)$$

$$e(\mathbf{x}) = \begin{cases} \frac{OT_{AC}}{s_1^{UB} + \varepsilon_1} - 1 \\ \frac{P_{AC}}{s_2^{UB} + \varepsilon_2} - 1 \end{cases} \quad (3-2-2)$$

The optimization variables need to be within physical limits or constraints to correspond with the problem requirements. Consequently, the optimization problem is implemented with box constraints and represented in the EQ 3-2-3 with the error function $e(\mathbf{z})$ having the same formulation as the EQ 3-2-2.

$$\mathbf{z}^* = \underset{\mathbf{z}}{arg \min} \max\{\dots e_k(\mathbf{z}) \dots\} \quad (3-2-3)$$

The optimization variables vector is re-formulated to the following equations:

$$\mathbf{x} = \begin{bmatrix} x_1 \\ x_2 \\ x_3 \end{bmatrix} = \begin{bmatrix} x_1^{lb} + (x_1^{ub} - x_1^{lb})(\sin z_1)^2 \\ x_2^{lb} + (x_2^{ub} - x_2^{lb})(\sin z_2)^2 \\ x_3^{lb} + (x_3^{ub} - x_3^{lb})(\sin z_3)^2 \end{bmatrix} \quad (3-2-4)$$

$$\mathbf{x}^{lb} = [32 \ 20 \ 1] \quad (3-2-5)$$

$$\mathbf{x}^{ub} = [55 \ 60 \ 10] \quad (3-2-6)$$

The optimization algorithm selected for this optimization problem is the Nelder-Mead method with 70 iterations as a maximum value, 700 evaluations of the function as a maximum value, 10% of function tolerance, and 10% of variable tolerance.

3.3. Results

The optimization algorithm was executed using the starting point $\mathbf{x}_0 = [33 \ 47 \ 1]^T$ converging to a solution represented on Equation (3-3-1)

$$\mathbf{x}^* = [54.9012 \ 30.3106 \ 1.7913]^T \quad (3-3-1)$$

The circuit response before and after the optimization process is shown in Figure 3-3-1, where the blue signal corresponds to the x_0 response and the red signal corresponds to the x^* response.

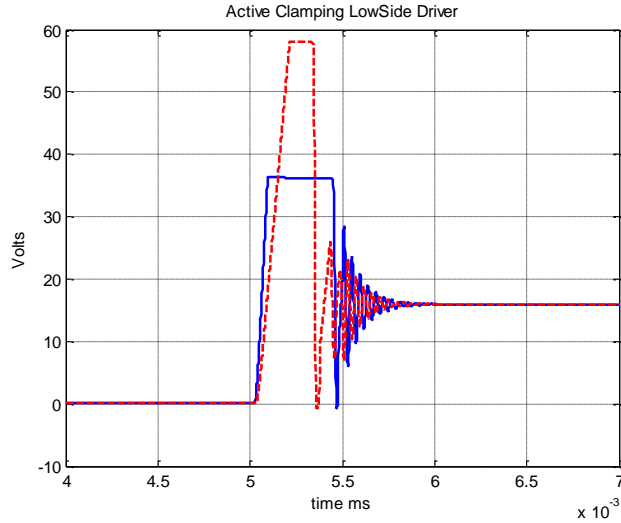


Figure 3-3-1. Active clamping circuit response using $x_0=[33 \ 47 \ 1]$ (blue) and x^* (red).

The power dissipation and ON time calculated using the solution x^* are $P_x^*=4.4871\text{mW}$ and $OT_x^*=126\mu\text{s}$. Consequently, the results satisfy the project requirements with the following performance details: function value at the solution $fval = 0.080070$, number of iterations of 54, number of function evaluations of 108 and exit flag of “*fminsearch converged to a solution*”.

Further test using multiple starting points were evaluated to check the stability of the optimization program.

3.4. Conclusions

The purpose of the current study was to implement an optimization algorithm to determine the proper components of the active clamping LSD circuit that satisfy the discharge time requirements with the minimum power dissipation. The Nelder-Mead optimization algorithm was selected using a minmax formulation with box constraints and a Manhattan norm for the error calculation.

The optimization algorithm converged to a solution that satisfied the requirements of the discharge time and power rating, using three different starting points to test diverse design scenarios. Consequently, it is important to point out that the design time could be reduced using the optimization algorithm to accomplish new requirements or product cost optimization projects by selecting the proper FET with a lower power rating, and therefore a lower price. Further research to reduce the variation of the clamping voltage due to the tolerance of components using an optimization of the results from the Monte Carlo analysis under different temperatures is suggested.

4. Conclusions

The present document summarizes the final projects concluded over the High Frequency Electronic Design concentration area. The objective of study of the three subjects was accomplished with the implementation of the optimization algorithm to determine the components of the Low Side Driver circuit with active clamping that satisfy the discharge time requirements with the minimum power dissipation. Besides the project development knowledge, multiple technical skills were learned and refined during the courses working hours. The mentioned skills played a key role for evolving my engineer mindset and problem solving.

In addition to the technical skills, multiple interpersonal skills were developed in order to plan and achieve the deliveries on time meanwhile it was attended all my family responsibilities with my two daughters and my wife.

In conclusion, it was an amazing journey that brings wealth on a personal as well as a professional level.

Appendix

A. FINAL PROJECT – BAND STOP FILTER

INTRODUCCIÓN

Se observa que la industria de las comunicaciones se está encaminando hacia las frecuencias de microondas, esto debido principalmente por el respectivo ancho de banda que se puede utilizar, ya que las bajas frecuencias actualmente están saturadas. Esto se ve reflejado en los servicios que se encuentran disponibles, tales como telefonía celular, localizadores de satélites, difusión de televisión o radio entre otras tecnologías.

En los servicios de microondas los equipos utilizados como celulares, televisión etc, se deben utilizar ciertos dispositivos que conectados entre sí determinen su funcionamiento y capacidades. Estos dispositivos normalmente cuentan con filtros, amplificadores, acopladores, resonadores etc. En particular un filtro es un dispositivo que permite el paso de cierto intervalo de frecuencia para el cual fue diseñado, y es el que limita el intervalo de frecuencias donde puede funcionar.

En este trabajo se va a documentar el proceso de diseño, construcción y funcionamiento de un filtro rechaza banda en tecnología microstrip (microcinta) en el cual se va a utilizar unos programas especializados en simulación electromagnética tales como Aplac y Sonnet. Este proyecto englobará los conocimientos obtenidos dentro del curso “Diseño de alta Frecuencia” impartido por el Dr. Zabdiel Brito Brito dentro de la institución del ITESO en la ciudad de Tlaquepaque Jalisco.

OBJETIVOS

Diseño, construcción y caracterización de un filtro rechaza banda Chebyshev de tercer orden con frecuencia central de 3.4GHz y ancho de banda fraccional de 5%.

Adicionales especificaciones técnicas:

- Tipo de respuesta de frecuencia : 0.1db Chebyshev
- Impedancia de referencia : 50Ω
- Rogers RO4003 (h= 0.81mm; cladding = 0.5 oz; er=3.55)

Para la verificación del correcto funcionamiento del filtro utilizar los siguientes simuladores electromagnéticos:

- Sonnet
- Aplac

Comparar los resultados obtenidos entre ambos simuladores así como comparar el funcionamiento de los filtros con los valores previamente calculados

MARCO TEÓRICO

1. MICROCINTA

Una microcinta es una línea de transmisión que consiste de una franja de metal y de un plano de tierra metálico separados por un dieléctrico, la cual se construye sobre una placa de metal. Esa se muestra en la figura 1.1 (a) y (b).

Donde h = Espesor del sustrato [m].

W_m = Ancho de la franja de metal [m].

t = Espesor de la franja de metal [m].

\mathcal{E} = Permitividad dieléctrica del sustrato [F/m].

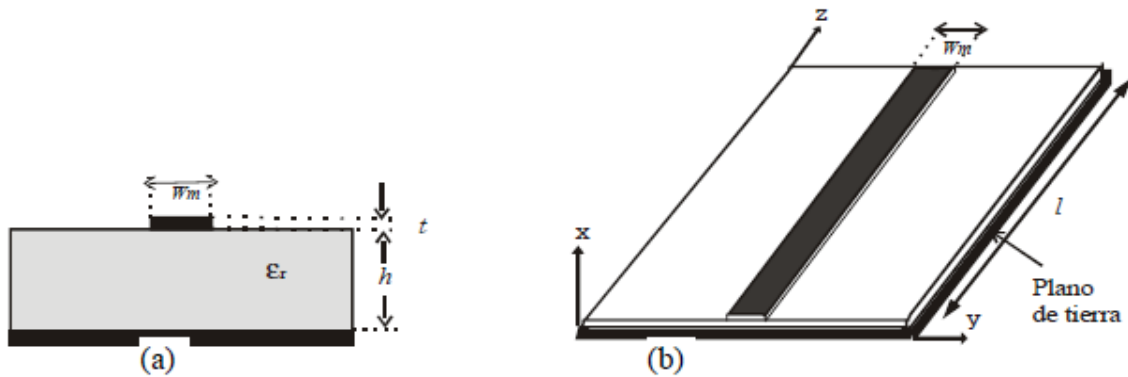


Figura 1.1 Microcinta. (a) Vista frontal. (b) Vista lateral

Normalmente \mathcal{E} se expresa en múltiplos de la permitividad dieléctrica del vacío $\mathcal{E}_0 = 8.854 \times 10^{-12}$ F/m², por lo que se define el parámetro de permitividad dieléctrica relativa dado por la ecuación 1.

$$\epsilon_r = \frac{\text{Permitividad del medio}}{\text{Permitividad del vacío}} = \frac{\mathcal{E}}{\mathcal{E}_0} \quad (1)$$

ϵ_r siempre tiene un valor mayor a 1.

La impedancia característica Z_0 de la microcinta es función de ϵ_r , h , W_m . Las ecuaciones para el cálculo de Z_0 son:

$$(2) \quad Z_0 = \begin{cases} \frac{(60/\sqrt{\epsilon_r}) \ln(8h/W_m + W_m/4h)}{120\pi} & \text{para } W_m/h \leq 1 \\ \frac{120\pi}{\sqrt{\epsilon_r} [W_m/h + 1.393 + 0.667 \ln(W_m/h + 1.444)]} & \text{para } W_m/h \geq 1 \end{cases}$$

Donde \mathcal{E}_e es la permitividad dieléctrica efectiva y está dada por

$$(3) \quad \mathcal{E}_e = \frac{\epsilon_r + 1}{2} + \frac{\epsilon_r - 1}{2} \frac{1}{\sqrt{1 + 12h/w_m}}$$

La razón $\frac{w_m}{h}$ está dada por:

$$(4) \quad \frac{w_m}{h} = \begin{cases} \frac{8e^A}{e^{2A} - 2} & \text{para } w_m/h < 2 \\ \frac{2}{\pi} \left[B - 1 - \ln(2B - 1) + \frac{\epsilon_r - 1}{2\epsilon_r} \left\{ \ln(B - 1) + 0.39 - \frac{0.61}{\epsilon_r} \right\} \right] & \text{para } w_m/h > 2 \end{cases}$$

Las constantes A y B se calculan con:

$$(5) \quad A = \frac{Z_0}{60} \sqrt{\frac{\epsilon_r + 1}{2} + \frac{\epsilon_r - 1}{\epsilon_r + 1} \left(0.23 + \frac{0.11}{\epsilon_r} \right)}$$

$$B = \frac{0.377\pi}{\sqrt{\epsilon_r}}$$

A las ecuaciones anteriores se les conoce como ecuaciones de síntesis. LAR

2. LINEAS DE TRANSMISION ACOPLADAS

Una línea de transmisión acoplada consta de dos tiras metálicas de longitud l , ancho w_m y separación s , las cuales se pueden construir sobre un sustrato dieléctrico de permitividad relativa \mathcal{E}_r y espesor h .

En la figura 2.1 (a) se muestra una vista lateral de esta estructura y en la figura 2.1 (b) una vista superior. El espesor t de la película conductora con la que está realizada tiene influencia en las pérdidas de energía que tienen las ondas a medida que se propagan a través de ella.

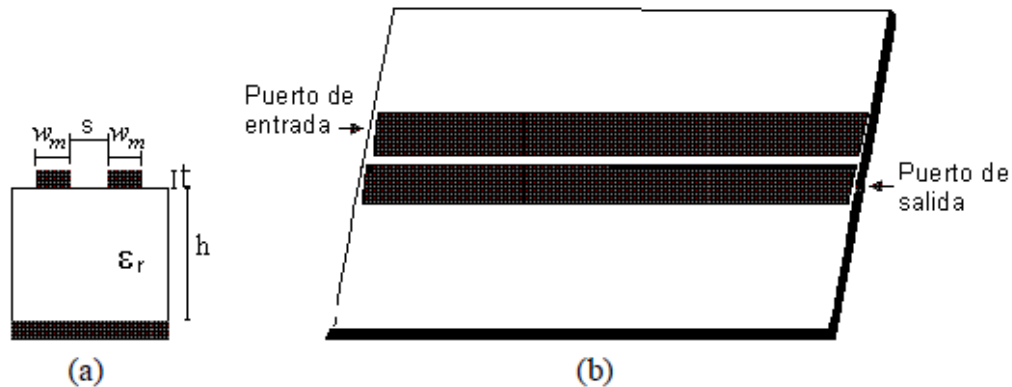


Figura 2.1 Línea de transmisión acoplada. (a) Vista Lateral. (b) Vista superior

El parámetro más importante de una línea de transmisión es la impedancia característica Z_0 , sin embargo, por la forma que tienen las líneas de transmisión acopladas presentan características particulares, que son:

- La impedancia característica es función de dos parámetros llamados impedancia par Z_{oe} e impedancia impar Z_{oo} .

- Como no existe contacto eléctrico entre las líneas parte de la energía que transporta una línea se induce en la otra y a esta razón se le llama factor de acoplamiento J .
- Todas las impedancias son función del ancho de las pistas W_m , la separación de las pistas s , el espesor del sustrato h y la permitividad dieléctrica relativa \mathcal{E}_r .

3. FILTROS CHEBYSHEV

Los filtros Chebyshev son filtros cuya característica es que en la banda de paso presenta máximos y mínimos en lugar de una respuesta plana pero en la banda de rechazo no presenta oscilaciones sino una respuesta plana. El número de máximos depende del orden del filtro, siendo el orden del filtro 2 veces la cantidad de máximos que presente; así, un filtro Chebyshev de tercer orden presentara un máximo y un medio. Un orden mayor también representa una atenuación más rápida. La atenuación que presentan los mínimos se le conoce como rizo y es igual a la atenuación de la frecuencia de corte.

La generación del filtro rechaza banda parte de los elementos del prototipo pasa bajas que se encuentran normalizados; tanto para “ $g_0=1$ ” y “ $W_0=1$ ”. Para cumplir los requerimientos del proyecto, en la Tabla 3.1 se muestran los elementos del prototipo pasa bajas Chebyshev con respuesta en frecuencia de 0.1 dB.

For passband ripple $L_{dr} = 0.1$ dB										
n	g_1	g_2	g_3	g_4	g_5	g_6	g_7	g_8	g_9	g_{10}
1	0.3052	1.0								
2	0.8431	0.6220	1.3554							
3	1.0316	1.1474	1.0316	1.0						
4	1.1088	1.3062	1.7704	0.8181	1.3554					
5	1.1468	1.3712	1.9750	1.3712	1.1468	1.0				
6	1.1681	1.4040	2.0562	1.5171	1.9029	0.8618	1.3554			
7	1.1812	1.4228	2.0967	1.5734	2.0967	1.4228	1.1812	1.0		
8	1.1898	1.4346	2.1199	1.6010	2.1700	1.5641	1.9445	0.8778	1.3554	
9	1.1957	1.4426	2.1346	1.6167	2.2054	1.6167	2.1346	1.4426	1.1957	1.0

Tabla 3.1 Prototipo L-P Chebyshev 0.1 dB.

La obtención de la reactancia normalizada utilizando los elementos del prototipo pasa bajas se realiza con la ecuación 6.

$$x_i = \omega_0 L_i = \frac{1}{\omega_0 C_i} = Z_0 \left(\frac{Z_U}{Z_0} \right)^2 \frac{g_0}{g_i \Omega_c FBW} \quad \text{for } i = 1 \text{ to } n \quad (6)$$

4. FILTRO RECHAZA BANDAS – TRANSFORMACIÓN

Un filtro rechaza banda permite la transferencia de energía de la fuente hasta la carga en dos bandas de frecuencia, una desde $f=0$ hasta la frecuencia de corte inferior, y otra desde la frecuencia de corte superior a una frecuencia de corte superior a una frecuencia infinita.

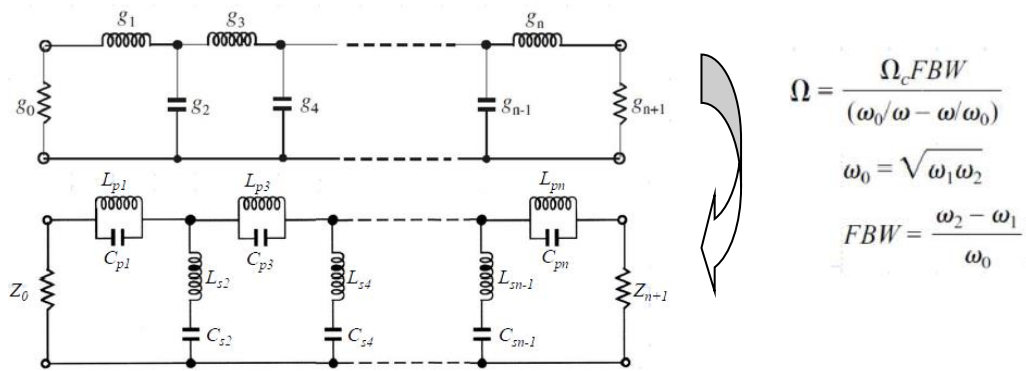


Figura 4.1 Transformación de filtro rechaza bandas

$$L_p = \left(\frac{\Omega_c FBW}{\omega_0} \right) \gamma_0 g$$

$$C_s = 1 / (\omega_0^2 L_p)$$

$$L_s = 1 / (\omega_0^2 C_s)$$

$$C_p = \left(\frac{\Omega_c FBW}{\omega_0} \right) \frac{g}{\gamma_0}$$

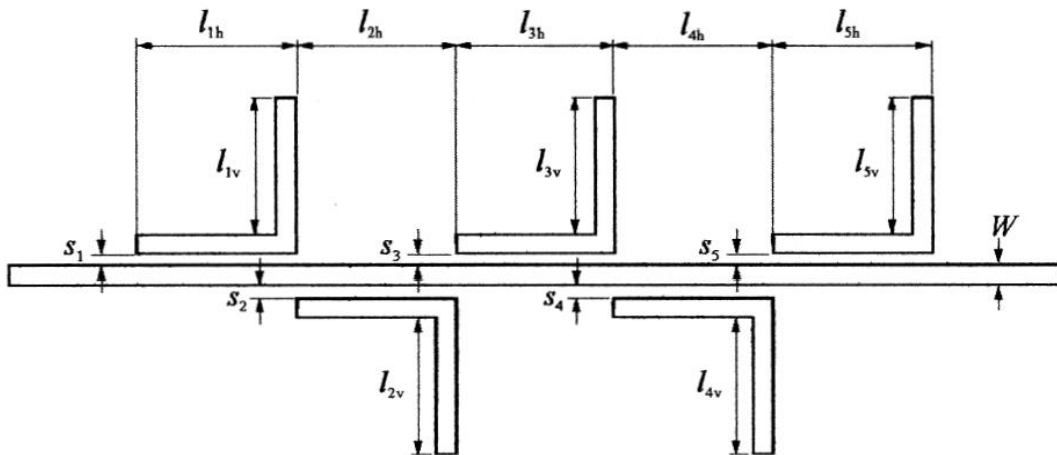


Figura 4.2 Transformación de filtro rechaza bandas usando Resonadores L

DISEÑO DEL FILTRO

A continuación se describirá el método seguido para la creación de un filtro rechaza banda que cumpla con las especificaciones de diseño previamente mencionados en la sección de objetivos. Este capítulo mencionara las siguientes etapas de diseño.

1. Simulación en Matlab
2. Creación de esquemático en APlac
3. Barrido de S en APlac para cada resonador
4. Integración de los tres resonadores en APLAC
5. Implementación del filtro en tecnología Microcinta en Sonnet
6. Barrido de S en Sonnet para cada resonador (L-section)
7. Integración de los tres resonadores en SONNET

5. SIMULACIÓN EN MATLAB

% Declaración de variables

```
c = 0.3e9; % Velocidad de la luz en espacio libre
(m/s).
fc=3.4e9; % Frecuencia
central
FBR=0.05; % Ancho de banda
fraccional
Zo=50; % Impedancia
característica
er=3.55; % Permitividad dieléctrica de
RO4003
H=0.81e-3; % Altura de
RO4003
```

% Cálculo de Constantes A y B acorde con la relación W_m/H

```
A=((Zo/60)*(((er+1)/2)^0.5))+(((er-1)/(er+1))*((0.23+(0.11/er)))); % Formula (5)
```

```
u=(8*exp(A))/(exp(2*A)-2); % Formula (4)
```

```
if (u<=2)
```

```
    A;
```

```
    u;
```

```
else
```

```
    B=(60*pi*pi)/(Zo*sqrt(er)); % Formula (5)
```

```
    u=(2/pi)*((B-1)-log((2*B)-1))+(((er-1)/(2*er))*(log(B-1)+0.39-(0.61/er)))); % Formula (4)
```

```
end
```

% Cálculo de permitividad dieléctrica efectiva

```
ere=((er+1)/2)+(((er-1)/2))*(((1+(12/u))^-0.5)); % Formula (3)
```

```
W=u*H
```

% Cálculo de velocidad de propagación y Longitud Eléctrica λ

```
vp = c/sqrt(ere);
```

```
lambda_Zo = vp/fc
```

% Frecuencia mínima y máxima a FBW = 5%

```
fmin = fc-((fc*FBR)/2)
```

```
fmax = fc+((fc*FBR)/2)
```

% Valores para rechaza bandas con Chebyshev $g_0 = 1.0$ $\Omega_c = 1$ $LAR = 0.1$ dB

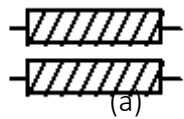
```
g0 = 1;  
g1 = 1.0316;  
g2 = 1.1474;  
g3 = g1;  
g4 = g0;  
X1_Z0 = g0 / (g1*1*FBR)  
X2_Z0 = g0 / (g2*1*FBR)  
X3_Z0 = g0 / (g3*1*FBR)  
Lquarts=lambda_Zo/4
```

Resultados:

W = 0.0018;	lambda_Zo = 0.0529;	fmin = 3.3150e+09;	fmax = 3.4850e+09;
X1_Z0 = 19.3874;	X2_Z0 = 17.4307;	X3_Z0 = 19.3874;	Lquarts = 0.0132;

6. CREACIÓN DEL ESQUEMÁTICO EN APLAC

Dado que APLAC es un simulador circuital, se requiere de un elemento específico que represente un acoplamiento magnético. MCLIN, Figura 6.1 (a), es un componente de APLAC que define una línea microcinta simétrica acoplada y que cuenta con 4 puertos, Figura 6.1 (b).



Example: Mclin "Mcl1" 2 1 2 3 4 W=0.6m S=0.2m L=20m

(b)



Figura 6.1 MCLIN (Symmetric coupled microstrip line)

MCLIN requiere parámetros de entrada para la definición del componente, los cuales están representados en la Tabla 6.2, así como parámetros del sustrato de la microcinta. En la Figura 6.3 se muestra la definición del sustrato ROGERS esto para cumplir con los requerimientos del proyecto tomando un modelo de simulación sin pérdidas.

Par	Arg	Description
	name	Name of the element
	m	Number of the coupled strips
	nii	Input node of the <i>i</i> th strip
	nio	Output node of the <i>i</i> th strip
L	x	Strip length <i>l</i>
S	x	Edge-to-edge distance <i>s</i> between adjacent strips
SEP	x	Alias of S
W	x	Strip width <i>w</i>

Tabla 6.2 Parámetros de entrada del componente MCLIN en APLAC.

```

MSub ROGERS
ER = 3.55
H = 0.81mm
TAND=0
LEVEL=1

```

Figura 6.3 Definición del substrato ROGERS

Paso previo a realizar el barrido paramétrico del espaciamiento entre las líneas acopladas, se realiza el armado del esquemático para una sola "L". En la Figura 6.4 se puede observar las conexiones realizadas sobre los puertos del componente MCLIN para lograr el prototipo en "L" de la línea acoplada y que se describe a continuación:

- El puerto 1 de MCLIN se conecta a una resistencia de $1000e^9 \Omega$ simulando un circuito abierto.
- El puerto 2 de MCLIN se conecta a un componente "Mloc" conformando así la "L" acoplada.
- El puerto 3 y 4 de MCLIN se conectan a la línea de transmisión.
- Puertos de entrada y salida a 50Ω con un barrido en frecuencia de 3GHz hasta 4.2 GHz.
- La longitud total de nuestro resonador "L" es la mitad de nuestra Longitud Eléctrica Lambda.

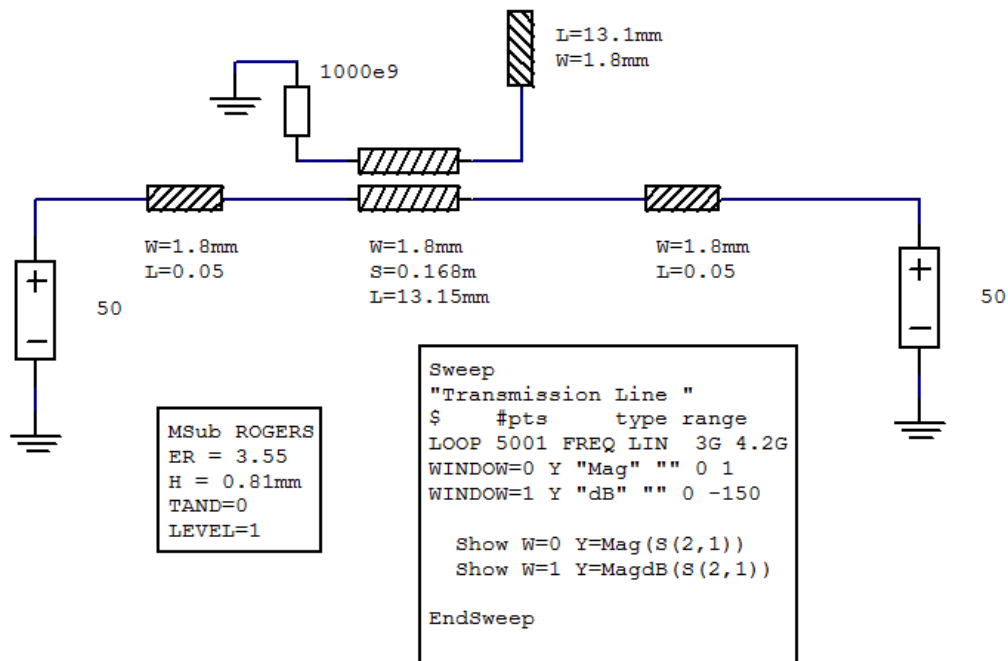


Figura 6.4 Esquemático en APLAC para realizar el barrido en “S”

7. BARRIDO DE S EN APLAC PARA CADA RESONADOR

La fórmula que relaciona los resultados de cada simulación con el valor de X_x/Z_0 se muestra en la Figura 7.1 (a). Para realizar la extracción de parámetros X/Z_0 en cada simulación de un “S” específico se utilizó el método descrito en la Figura 7.1 (b).

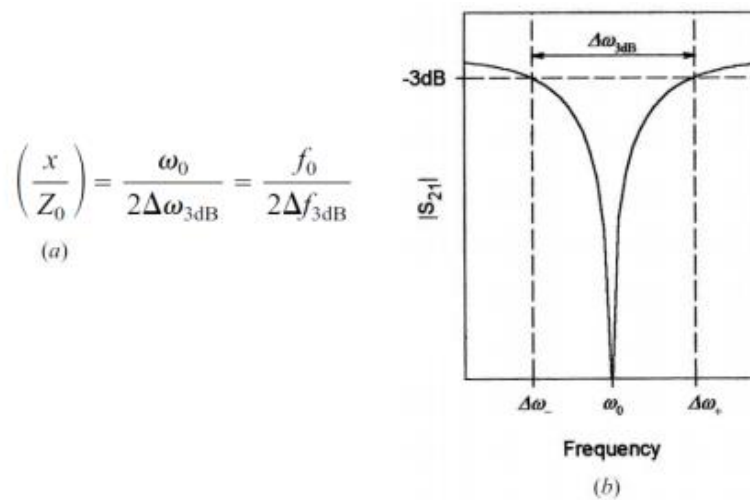


Figura 7.1 (a) Fórmula para relacionar x/Z_0 y la respuesta en frecuencia. (b) Ejemplo de medición.

Primeramente un **barrido burdo en "S"** fue realizado para encontrar los puntos de interés donde $Xx/Z0$ se acerca a nuestros resultados obtenidos en MATLAB para $X1/Z0=19.38$ y $X2/Z0=17.43$. Los resultados son mostrados en la Tabla 7.2 y la Grafica 7.3; marcando en verde los puntos de interés.

Fmin(3dB)	Fmax(3dB)	F0	Xx/Z0	Valores de S
3.34	3.453	3.394	15.0176991	0.1
3.342	3.45	3.394	15.712963	0.11
3.344	3.447	3.394	16.4757282	0.12
3.346	3.445	3.393	17.1363636	0.13
3.347	3.442	3.393	17.8578947	0.14
3.349	3.44	3.393	18.6428571	0.15
3.35	3.438	3.392	19.2727273	0.16
3.351	3.436	3.392	19.9529412	0.17

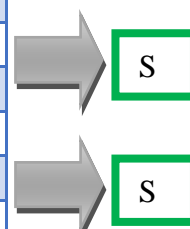
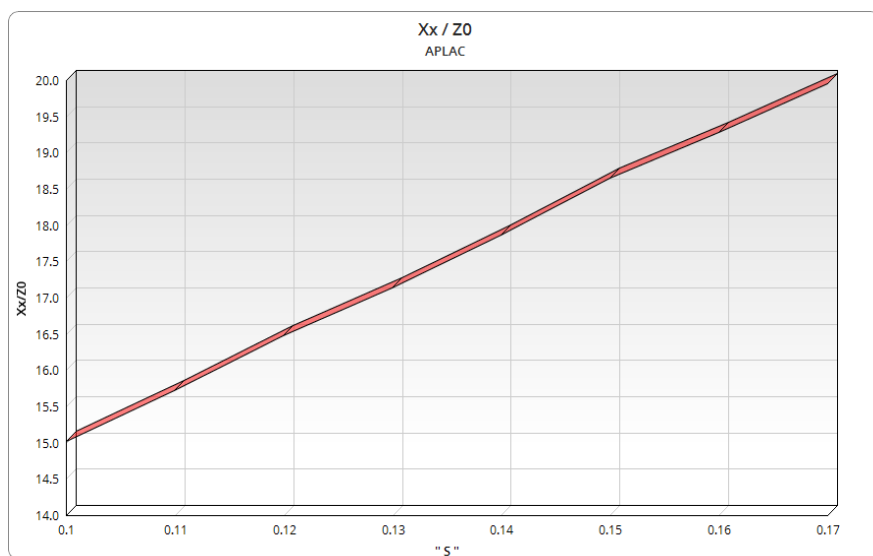


Tabla 7.2 Barrido burdo sobre "S" en APLAC

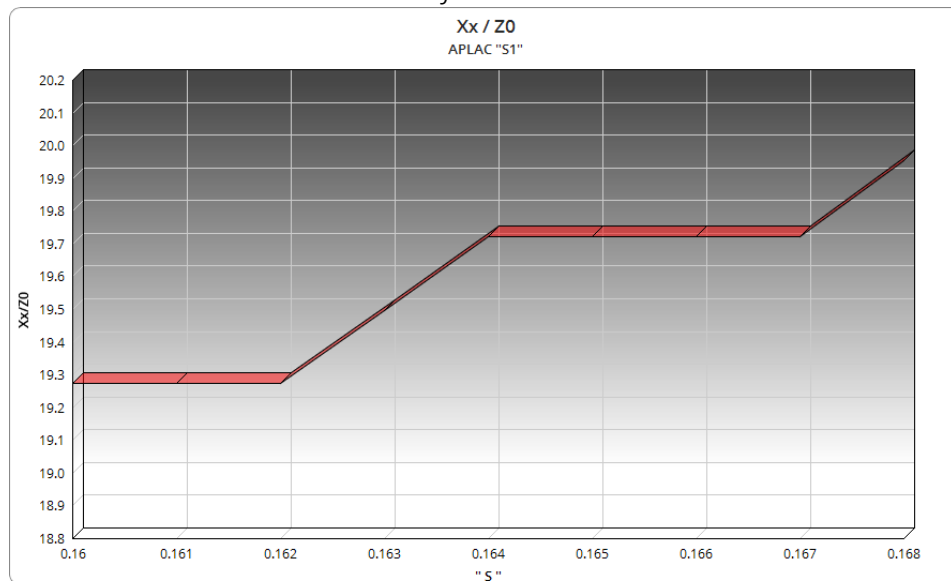


Grafica 7.3 Barrido burdo sobre "S" en APLAC

Un **barrido más fino en "S1"** es realizado sobre el rango de interés ($0.16 < S1 < 0.17$) para localizar el punto más cercano posible en donde $X1/Z0=19.38$, obteniendo los resultados mostrados en la Tabla 7.4 y la Gráfica 7.5. Se remarca en verde los puntos más cercanos entre los cuales estará el valor deseado y sobre el cual se tratarán de hacer los ajustes finales al momento de acoplar los tres resonadores.

FBW		Target	S1 = 19.38	
Fmin(3dB)	Fmax(3dB)	F0	Xx/Z0	Valores de "S"
3.35	3.438	3.392	19.2727273	0.16
3.35	3.438	3.392	19.2727273	0.161
3.35	3.438	3.392	19.2727273	0.162
3.35	3.437	3.392	19.4942529	0.163
3.351	3.437	3.392	19.7209302	0.164
3.351	3.437	3.392	19.7209302	0.165
3.351	3.437	3.392	19.7209302	0.166
3.351	3.437	3.392	19.7209302	0.167
3.351	3.436	3.392	19.9529412	0.168

Tabla 7.4 Barrido fino sobre "S1" en APLAC

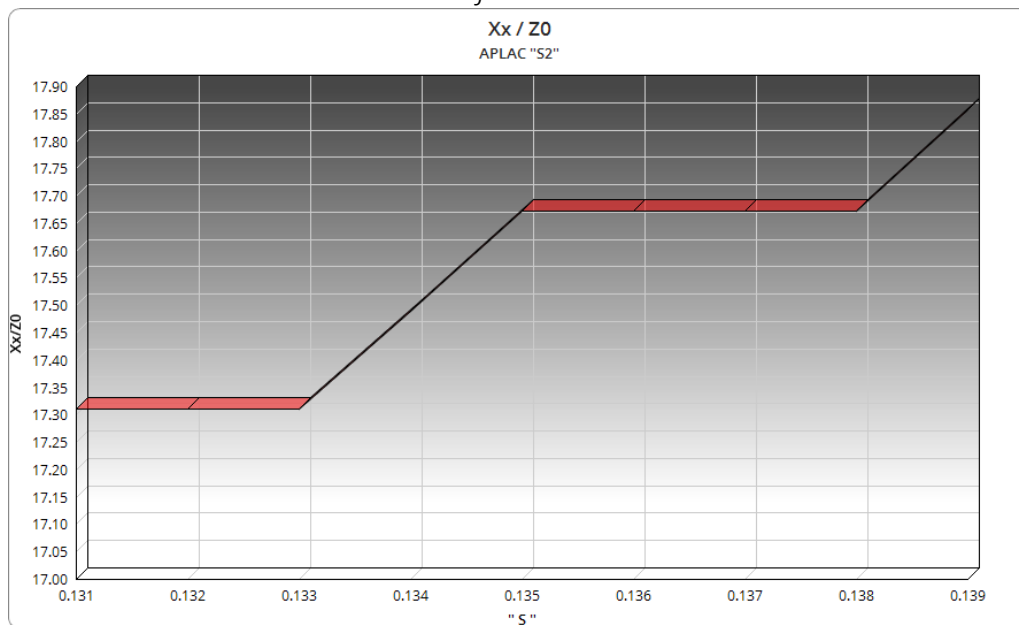


Gráfica 7.5 Barrido fino sobre "S1" en APLAC.

A continuación se realiza el **barrido fino en "S2"** sobre el rango $[0.13 < S2 < 0.14]$ obteniendo los resultados mostrados en la Tabla 7.6 y la gráfica 7.7; remarcando en verde los valores de "S" donde se obtiene el valor de $X2/Z0$ más cercano a 17.43.

FBW		Target	S2 = 17.43	
Fmin(3dB)	Fmax(3dB)	F0	Xx/Z0	Valores de "S"
3.346	3.444	3.393	17.3112245	0.131
3.346	3.444	3.393	17.3112245	0.132
3.346	3.444	3.393	17.3112245	0.133
3.347	3.444	3.393	17.4896907	0.134
3.347	3.443	3.393	17.671875	0.135
3.347	3.443	3.393	17.671875	0.136
3.347	3.443	3.393	17.671875	0.137
3.347	3.443	3.393	17.671875	0.138
3.347	3.442	3.393	17.8578947	0.139

Tabla 7.6 Barrido fino sobre "S2" en APLAC



Gráfica 7.7 Barrido fino sobre "S2" en APLAC.

En base a los gráficos previamente encontrados los valores seleccionados para realizar la integración de los tres resonadores son:

- S1= 0.162 mm
- S2= 0.133 mm
- S3= 0.162 mm

8. INTEGRACIÓN DE LOS TRES RESONADORES EN APLAC

La separación entre el punto medio de cada resonador y el siguiente tiene que ser de un cuarto de la medida de longitud eléctrica λ , razón por la cual se decidió establecer la longitud del brazo inferior como $\lambda/4 = 13.15 \text{ mm}$ y tener los tres resonadores uno tras otro, formando así la separación requerida por el tipo de filtro. En la Figura 8.1 se muestra el esquemático del filtro Rechaza Bandas de tercer orden Chebyshev 0.1 dB.

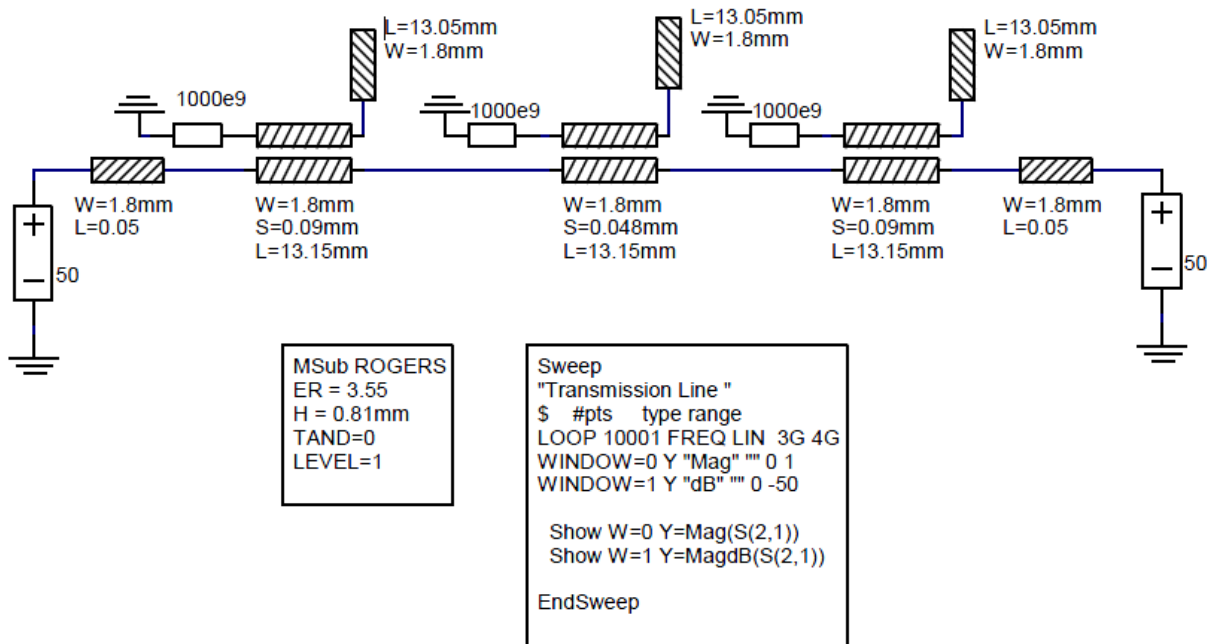


Figura 8.1 Esquemático del Filtro Rechaza Banda Chebyshev 0.1 dB

Nota: Los valores de "S" mostrados en la figura no concuerdan con los obtenidos en el barrido paramétrico. La razón se explicará en los siguientes párrafos.

Los resultados obtenidos al correr la simulación no fueron los esperados, ya que se obtuvo un Ancho de Banda Fraccional (FBW por sus siglas en ingles) de 118 MHz, siendo que el requerimiento era de 5% de F_0 ; 170MHz. Para solucionar lo anterior se realizaron "ajustes finos" sobre los valores de "S" para ampliar el FBW.

La siguiente tabla nos muestra los valores con los que se logró obtener el FBW del 5% y la F_0 de 3.4GHz de forma individual y de forma conjunta hablando del acoplamiento de los tres resonadores "L"

Valores finales obtenidos para S1, S2, S3			
"S"	Valor del barrido	Valor Ajustado	Relación de reducción
S1 = S3	0.162	0.09	1.8
S2	0.133	0.048	2.77

Tabla 8.2 Diferencias entre el barrido de "S" y la simulación final.

Ajustados los valores de “S” se obtienen las gráficas de la simulación mostrando que los requerimientos son cumplidos. En la Figura 8.3 se puede observar la frecuencia central F_0 a 3.4 GHz, mostrada en los cursores en la parte superior de la figura.

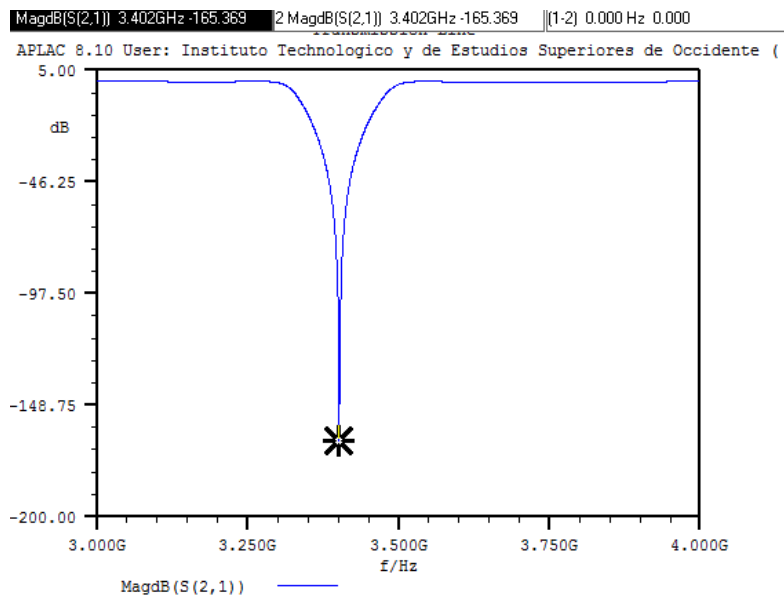


Figura 8.3 Frecuencia central del filtro Rechaza Bandas Chebyshev 3^{er} orden.

El FBW de 170MHz es mostrado en la parte superior derecha como la diferencia entre los dos cursores de la Figura 8.4

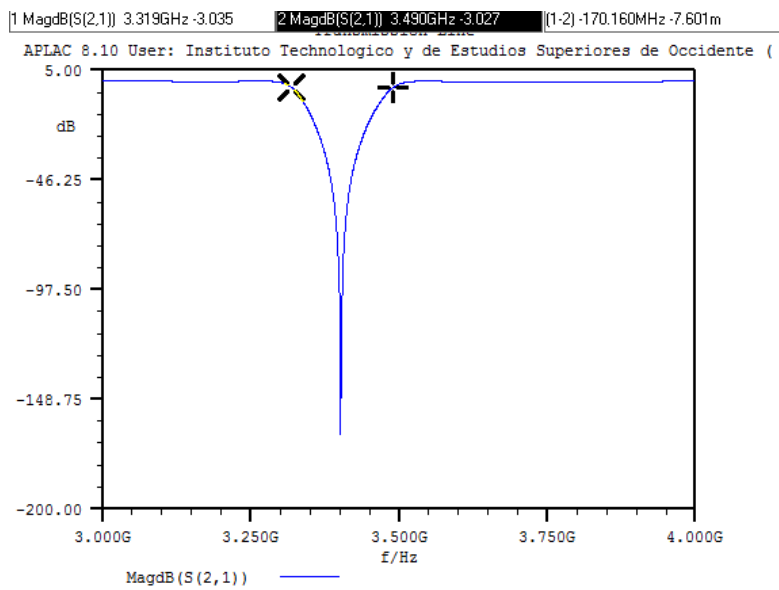


Figura 8.4 FBW del filtro Rechaza Bandas Chebyshev 3^{er} orden.

9. IMPLEMENTACIÓN DEL FILTRO EN TECNOLOGÍA MICROCINTA EN SONNET

La definición de los “Dielectric Layers” de SONNET se tiene que hacer siguiendo los requerimientos de ROGERS dictados en los Objetivos de este proyecto. En la Figura 9.1 se tiene la definición utilizada en SONNET para realizar la simulación. La capa de aire se define de 5 mm y la metalización se declaró sin pérdidas (LOSSLESS en inglés). Un barrido en frecuencia fue seleccionado en esta simulación como lo muestra la Figura 9.2.

	Thickness (mm)	Mat. Name	Erel	Dielectric Loss Tan	Cnd, Res S/m, Ohm-cm
0	5.0	Air	1.0	0.0	Cnd:0.0
GND	0.81	ROGERS	3.55	0.0	Cnd:0.0

Figura 9.1 Configuración de “Dielectric Layers” para ROGERS en SONNET.

Analysis Control

Adaptive Sweep (ABS)

Start (GHz): 3.0

Stop (GHz): 4.0

Figura 9.2 Barrido en frecuencia para SONNET.

10. BARRIDO DE S EN SONNET PARA CADA RESONADOR (L-SECTION)

A diferencia de APLAC, en SONNET se realizó el diseño del "Layout" con las medidas requeridas para realizar el barrido en "S".

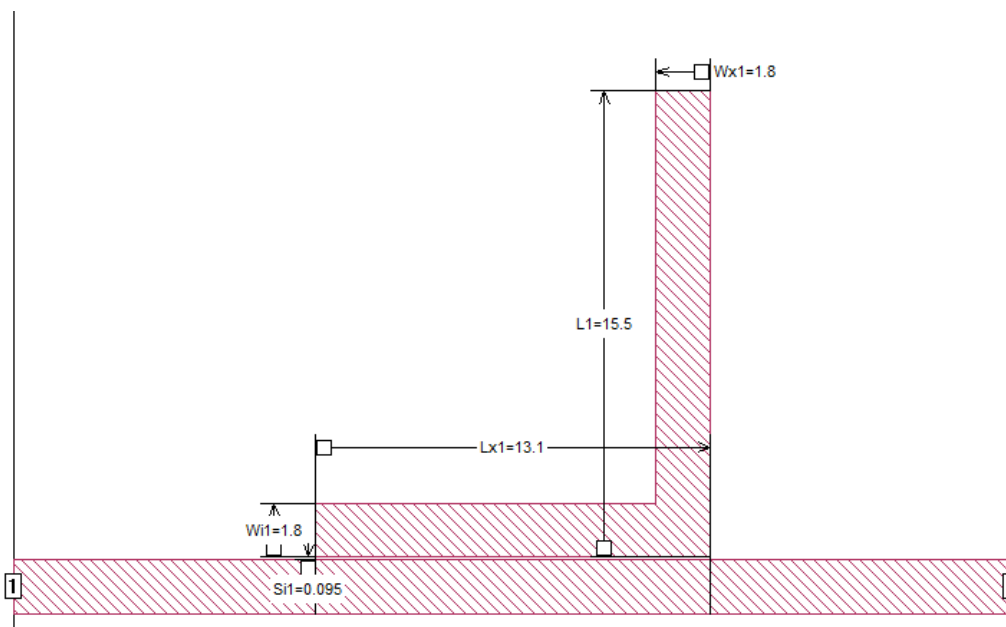


Figura 10.1 Layout en SONNET para el barrido de "S".

Se puede notar que el valor de L1 es de 15.5 mm y esto se debe a que se tiene que agregar el ancho del brazo inferior al valor de cuarto de Lambda. En APLAC no era necesario, ya que no se contaba con el componente acoplado en forma de codo para unir los dos brazos de la "L".

Con los datos anteriores se procede a realizar el **barrido burdo en "S"** con SONNET y obtener así los puntos de interés mostrados en la Tabla 10.2 y la Gráfica 10.3. Se marca en verde los rangos donde se encuentran los valores de $Xx/Z0$ que más se acercan a los valores calculados.

Fmin(3dB)	Fmax(3dB)	F0	Xx/Z0	Valores de S
3.345	3.474	3.408	13.2093023	0.05
3.355	3.45	3.405	17.9210526	0.1
3.37	3.447	3.41	22.1428571	0.15
3.367	3.43	3.395	26.9444444	0.2
3.373	3.426	3.399	32.0660377	0.25
3.378	3.423	3.4	37.7777778	0.3

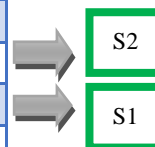
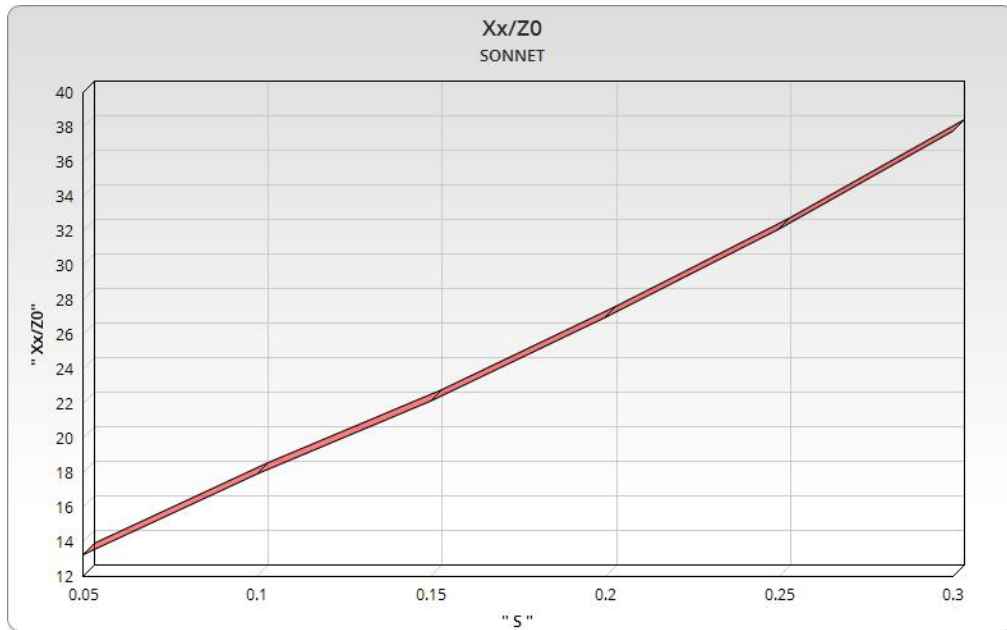


Tabla 5.6 Barrido burdo sobre "S" en SONNET

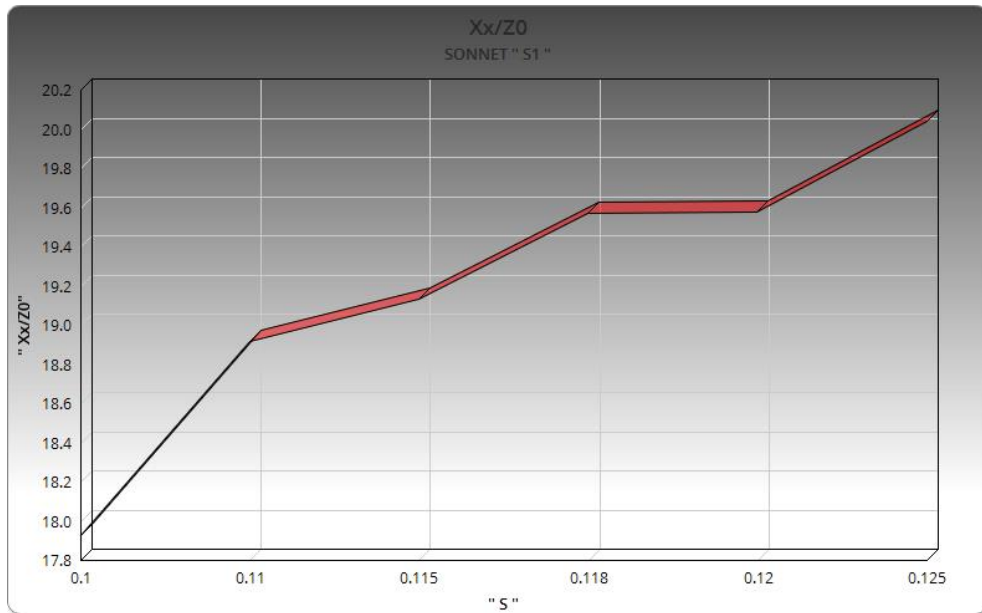


Gráfica 10.3 Barrido burdo sobre "S" en SONNET

Con los rangos de interés obtenidos en el anterior barrido se prosigue a hacer un **barrido fino sobre "S1"** en el rango $[0.1 < S1 < 0.125]$. En la Tabla 10.4 se puede observar que el valor de $X1/Z0=19.38$ se cumple dentro del rango de $0.115 < S1 < 0.118$. También se debe de notar que los incrementos en los puntos del barrido no son simétricos y esto se debe al "grid" utilizado en SONNET para realizar las simulaciones.

FBW		Target	S1 = 19.38	
Fmin(3dB)	Fmax(3dB)	F0	Xx/Z0	Valores de "S"
3.355	3.45	3.405	17.9210526	0.1
3.36	3.45	3.405	18.9166667	0.11
3.361	3.45	3.405	19.1292135	0.115
3.362	3.449	3.405	19.5689655	0.118
3.363	3.45	3.406	19.5747126	0.12
3.364	3.449	3.406	20.0352941	0.125

Tabla 10.4 Barrido fino sobre "S1" en SONNET

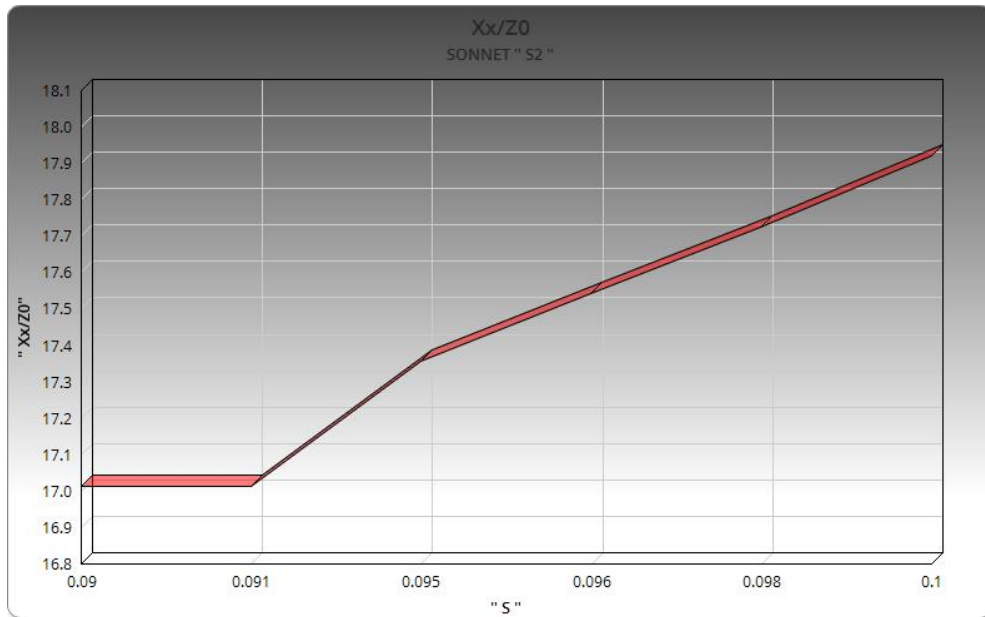


Gráfica 10.5 Barrido fino sobre "S1" en SONNET.

Solo resta hacer un barrido fino sobre el rango $[0.09 < S2 < 0.1]$ en "S2" para obtener el valor más cercano a 17.43 de $X2/Z0$.

FBW		Target	S2= 17.43	
Fmin(3dB)	Fmax(3dB)	F0	Xx/Z0	Valores de S
3.353	3.453	3.402	17.01	0.09
3.353	3.453	3.402	17.01	0.091
3.354	3.452	3.402	17.3571429	0.095
3.355	3.452	3.403	17.5412371	0.096
3.356	3.452	3.403	17.7239583	0.098
3.355	3.45	3.405	17.9210526	0.1

Tabla 10.9 Barrido fino sobre "S2" en SONNET



Gráfica 10.10 Barrido fino sobre "S2" en SONNET.

En base a los gráficos anteriores los valores seleccionados para realizar la integración de los tres resonadores son:

- S1= 0.115 mm
- S2= 0.095 mm
- S3= 0.115 mm

11. INTEGRACIÓN DE LOS TRES RESONADORES EN SONNET

Al igual que en APLAC la separación entre el punto medio de cada resonador y el siguiente tiene que ser de un cuarto de la medida de longitud eléctrica Λ , razón por la cual se decidió establecer la longitud del brazo inferior como $\Lambda/4 = 13.15 \text{ mm}$ y tener los tres resonadores uno tras otro, formando así la separación requerida por el tipo de filtro. En la Figura 11.1 se muestra el layout del filtro Rechaza Bandas de tercer orden Chebyshev 0.1 dB.

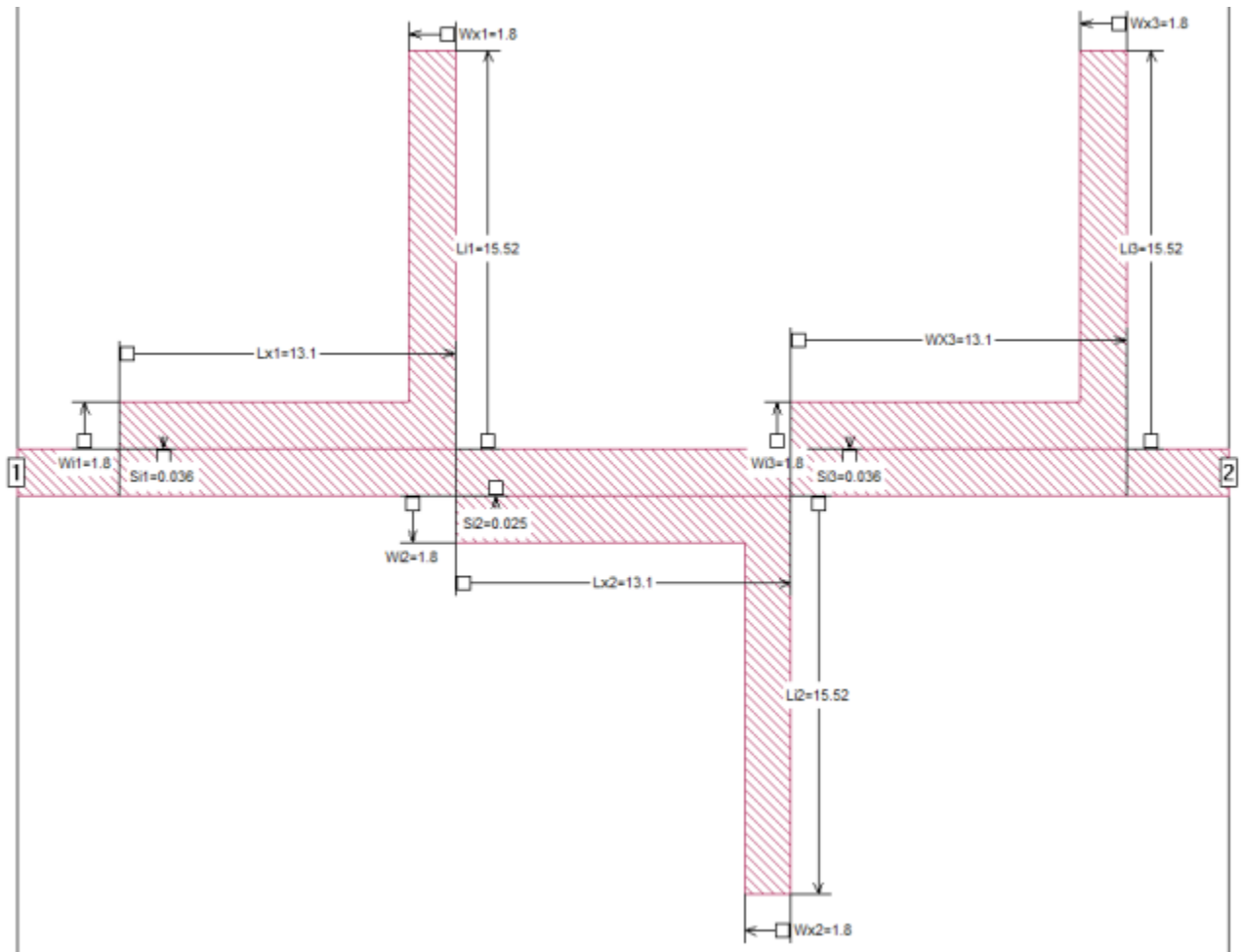


Figura 11.1 Layout filtro Rechaza Banda Chebyshev 3er orden

Nota: En SONNET se tiene un comportamiento similar a APLAC, en donde al hacer la integración de los tres resonadores y simular, no se obtiene el ancho de banda fraccional requerido del 5% ni la F_0 de 3.4Ghz. Se debe notar en la Figura 11.1 que los valores de "S" no son los resultantes del barrido paramétrico.

La siguiente Tabla 11.2 nos muestra los valores con los que se logró obtener el FBW del 5% y la F_0 de 3.4GHz.

Valores finales obtenidos para S			
"S"	Valor del barrido	Valor Ajustado	Relación de reducción
S1_S3	0.115	0.036	3.19
S2	0.095	0.025	3.8

Tabla 11.2 Diferencias entre el barrido de "S" y la simulación final con SONNET

Con los valores ajustados de "S" se procede a obtener las gráficas de simulación que nos permitan demostrar que se cumplen los requerimientos previamente establecidos.

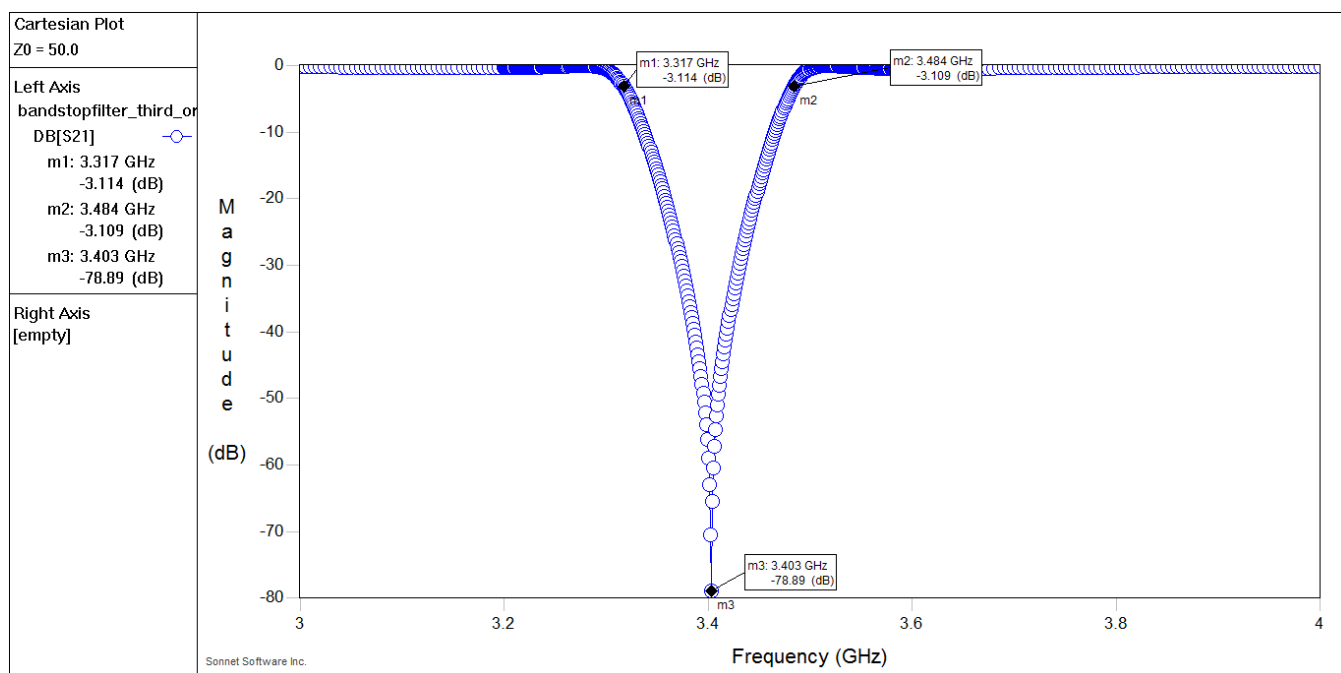


Figura 11.3 Respuesta en frecuencia del filtro Rechaza Bandas Chebyshev 3^{er} orden.

La frecuencia central de los resultados de simulación es de **3.403 GHz**, como se muestra en la Figura 11.3 con el marcador "m3" en la parte central inferior de la imagen. Con los marcadores "m1" y "m2" en las frecuencias de 3.317GHz y 3.484GHz (3dbs) respectivamente, podemos obtener el FBW que es de **167MHz**.

CONCLUSIONES

Con ayuda de este proyecto se logró obtener el conocimiento adecuado para el desarrollo de un filtro Rechaza Bandas en una tecnología de microcinta respetando los requerimientos de funcionamiento previamente establecidos, además del desarrollo de habilidades para la realización de las pruebas y ajustes necesarios en los simuladores electromagnéticos adecuados.

Durante el desarrollo del filtro se presentaron muchos desafíos y aprendizajes de los cuales podemos enumerar los siguientes:

1. El simulador circuital utilizado, APLAC, fue un problema porque debido a que es un poco obsoleto, presentaba algunas fallas de licencia en los laboratorios del ITESO. Lo anterior obstaculizó el desarrollo del proyecto, ya que las horas productivas de uso del simulador fueron disminuidas alrededor del 90%. Por lo que se recomienda utilizar otro simulador para futuros cursos.
2. Nos percatamos que cada uno de los parámetros (distancia "S", longitud del resonador, dimensiones de la caja en SONNET, Dieléctrico del Aire, pérdidas del material) afectaban de manera directa el funcionamiento del filtro. La frecuencia central está directamente relacionada con la longitud del resonador y a lo largo de las pruebas se tuvo que estar ajustando la longitud total del resonador para obtener la frecuencia central deseada y de lo contrario la distancia "S" es el parámetro que más influencia tiene en el FBW. Además, cabe destacar que es de suma importancia la impedancia de las líneas de transmisión y también así del resonador por lo que el parámetro destacado es "W" dada las características del substrato. La configuración de los simuladores, tal como dimensiones de la caja, pérdidas del material y dieléctrico del aire; son factores que tienen que ser tomados en cuenta y establecidos de manera adecuada para tener una respuesta más limpia y evitar cualquier tipo de resonancias.
3. El comportamiento de los resonadores de manera individual difiere a los resultados obtenidos al integrar los tres resonadores; por lo cual el barrido de "S" fue muy importante para así lograr indicar el punto sobre el cual se comenzaría a ajustar el filtro en relación de una tercera parte del los valores originales obtenidos en el barrido.
4. El diseño en SONNET difiere un poco contra los resultados de APLAC, atribuimos este comportamiento a que APLAC no existe un componente que simule enteramente el acoplamiento de una "L"; por lo tanto el codo que une el brazo inferior con el brazo superior de la "L" no se acopla en la simulación. En cambio en SONNET se realiza el diseño en "LAYOUT" de la figura completa "L", teniendo así más área de acoplamiento y por lo tanto el área cubierta es mayor y difieren los resultados.

BIBLIOGRAFÍA

-APLAC Online Documentation

-Manuals for APLAC

-D. M. Pozar, Microwave Engineering, Wiley, 2005

- Widiastuti, Dian & Yansyah, Ferdi & Alaydrus, Mudrik. (2016). Bandstop Filter for Radar Application with L Resonator.

B. MONTECARLO ANALYSIS OF AN ACTIVE CLAMPING CIRCUIT IN A LOW SIDE DRIVER POWER OUTPUT

INTRODUCTION

The intention of this project is to perform a Monte Carlo Analysis (MCA) in an Active Clamping Circuit. This circuit is used in a Low Side Driver (LSD) Power Output to accelerate the current decay of an inductive-resistive valve. In general the LSD creates a path to ground for the load when it is active and can be toggled at different Frequencies and Pulse Width Modulation in order to get the desired current at the load.

Power outputs are used in automotive in order to control valves such as the Fuel Pump or the Starter of the engine. It is very important to check the correct population of all the components of this circuitry and also the correct functionality as it will control important features of the vehicle.

The purpose of this project is the analysis of the behavior of the Clamping voltage when the LSD is turned OFF varying all the components according to the specified tolerance and modifying the Temperature. The engine could be operating among different ranges of temperature, so the MCA is executed at three different temperatures.

A brief explanation of the LSD operation is reported in the Theory section in order to give to the reader the basic knowledge about this Power Output and the expected response over the transient response.

It is very important to check all the components and correct functionality of the Electronic Controller Unit. This project helps to check if the limits given by the Worst Case Analysis are correct and can guarantee that a bad component or wrong population could be caught at a functional test.

Theory

The Low Side Driver is a circuit that provides a path to Ground to a specific load. It uses a N-channel MOS with source connected to ground. The basic schematic for a LSD is shown at Figure 1.

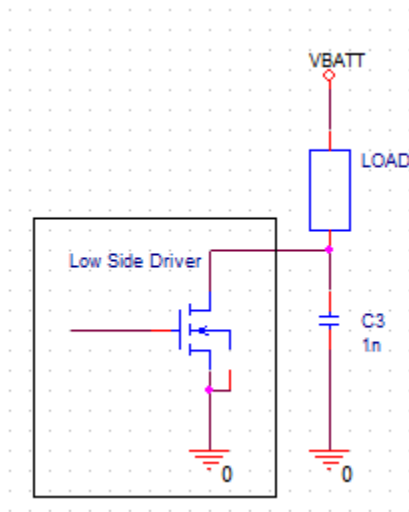


Figure 1.

Different Loads can be used with a LSD in order to control the current flowing to ground switching the Mosfet. Examples of these loads are relays, valves, solenoids and heaters. The circuitry to be analyzed at this project is shown at Figure 2.

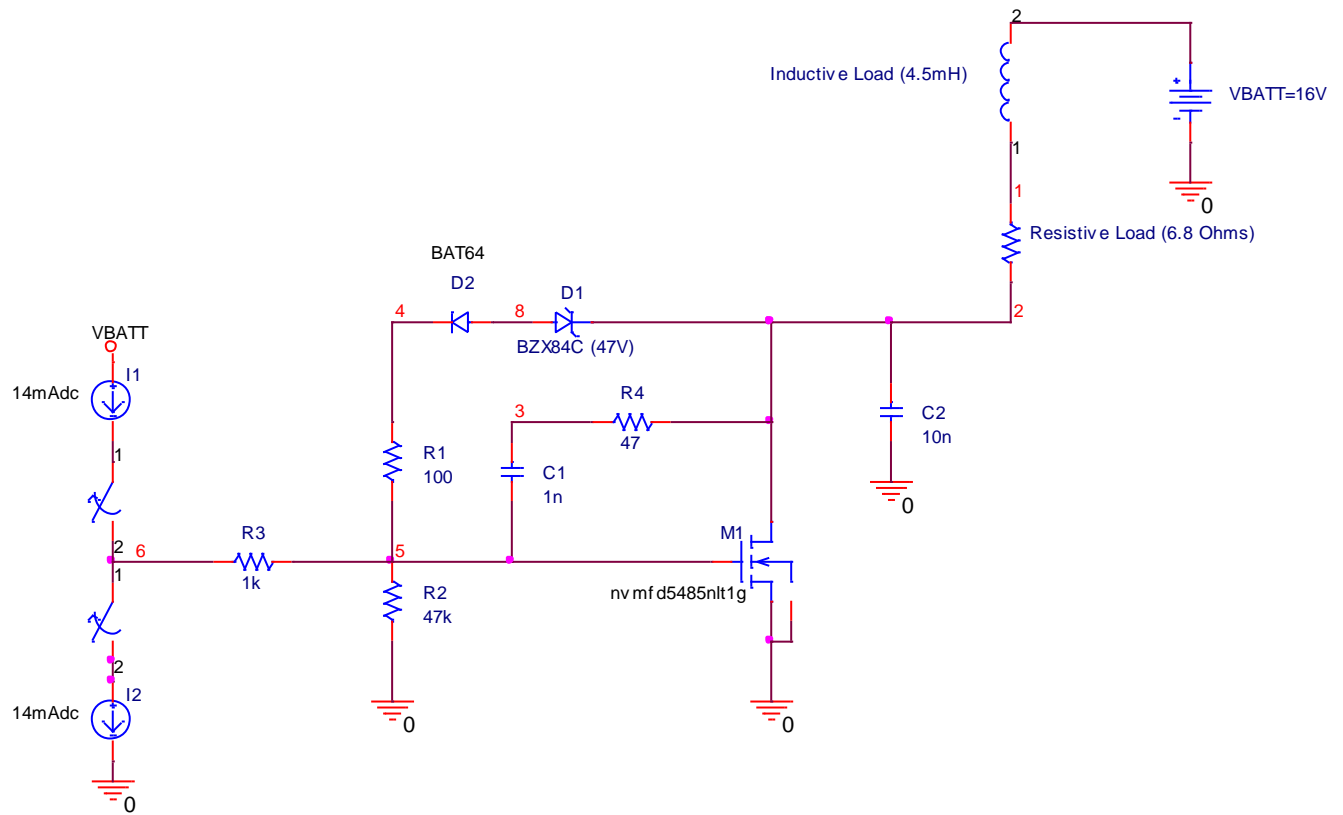


Figure 2.

This is the explanation of how the circuit works: M1 Mosfet is used to create the path to ground for the load, so when it is turned ON the current start to increase and takes some time in order to reach the maximum current given by the resistive part of the load if the duty cycle of the ASIC driver allows it.

$$I_{max} = \frac{V_{batt}}{R(load)} \quad Eq1.$$

The mosfet is activated by a pre-driver (ASIC) that handles the activation profile and another functionalities as the diagnostic of the power stage (not represented in Figure 2). The ASIC is represented with the two current sources, I1 and I2, that allows the pre-driver to turn ON or OFF the FET.

When the FET is ON, the current is flowing through the load and energy is stored in the inductor as magnetic field. When the FET is turned OFF, the inductor starts increasing its voltage in order to find a way to discharge all this energy. The inductor finally finds a way to discharge a little current breaking the V_b of the Zener D1 and flowing to ground through R1, R2 and the gate of the M1 (See Figure 3).

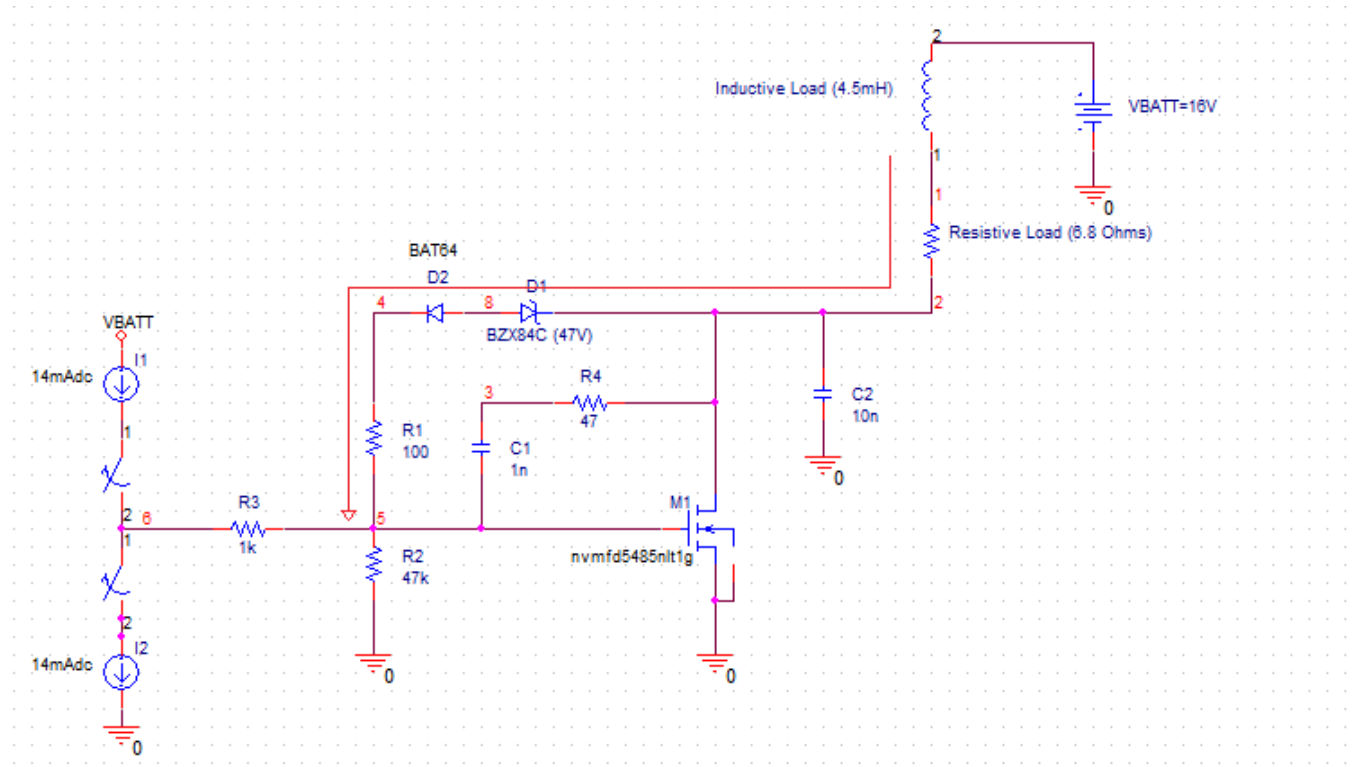


Figure 3.

At the same time the branch across the Zener D1 will activate the FET M1 and starting discharging a little bit the inductor through the M1 drain to ground. But this will decrease the inductor voltage below the V_b of D1, cutting off the branch described and turning the FET M1 OFF. With the FET in OFF state the inductor will start to increase its voltage again to reach the V_b of D1 threshold. The circuit will be playing turning ON and OFF the FET moving the inductor voltage and at the same time discharging the energy. This is called “Active Clamping”.

This cycle will be repeated in a control closed loop, with the M1 FET playing in the non-linear zone (Ohmic region) and discharging the inductor across the M1 drain and setting a voltage at node 2 given by the following:

$$V(2) = V_z + V_f + V(R1) + V_{plateau}(M1) \quad \text{Eq.2}$$

Where:

- Vz=Vbreak voltage of the Zener D1
- Vf=Forward voltage of D2
- V(R1)=Voltage droop over R1
- Vplateu(M1)= Plateu voltage of M1

The plateau voltage is the VGS voltage when the FET starts to conducting and entering into the Ohmic Region. In Figure 4 the plateau voltage is the flat area of VGS vs the Gate Charge.

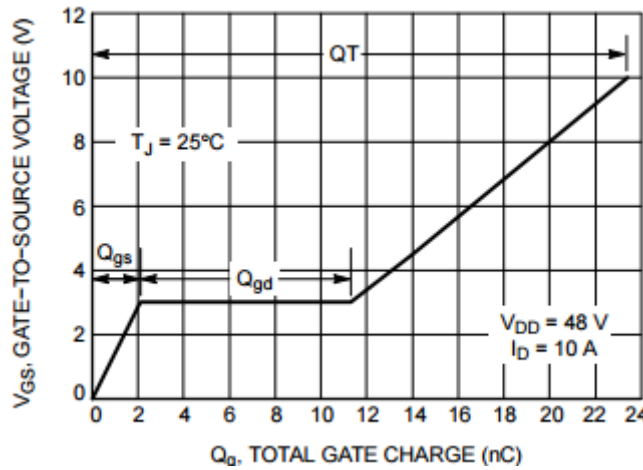


Figure 4.

The plateau voltage is dependent of the construction process of the mosfet and will vary from each silicon wafer to another. A good approximation taken from design team is $2.4 < V_{plateu} < 3.4$. A good way to estimate this value from a given mosfet is explained in this documente from TI: “Estimating MOSFET Parameters from the Data Sheet”. Web page link stated in the Bibliography.

So taking Vz=47v, Vf=0.6v, Vplateu=3v :

$$V(R1) = \frac{V_{plateu}}{R2 || R3} * R1 = 306mV$$

$$V(2) = 47 + 0.6 + 0.306 + 3 = 50.906V$$

This V(2)=50.906V is the nominal response for the Active Clamping Voltage at 25°C.

Experiment

The circuit of Figure 2 was implemented in a SPICE file and mounted over a Matlab driver function in order to receive specific parameters, run the with WINSPIICE, save the result in a*.csv file and return the transient analysis to the call function. Please refer to Appendix "1.-".

The file was executed once in order to corroborate that circuit was properly described at SPICE and it is working as expected. In figure 5, the voltage at V(2) (Upper picture) and current over the load (Lower picture) are shown.

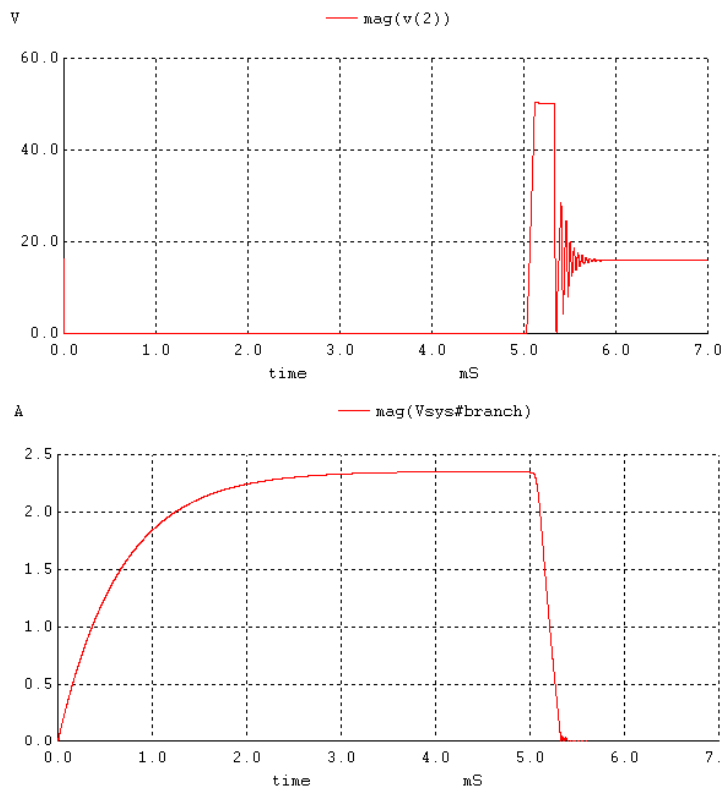


Figure 5.

From Figure 5, we can ensure that the circuit is working good turning the FET between 0 and 5ms, having a current through the load around 2.35A. When the FET is turned OFF at 5ms, the Clamping voltage over the plot is around 50V and the current decrease to 0 Amps before 500us.

After checking that the circuit is working as expected, it was developed the code for the Monte Carlo Analysis (refer to Appendix "2.-") The components are varied following the tolerances shown in Table 1 and following a Gaussian distribution.

Component	Value	Tolerance
R1	100 Ω	5%
R2	4700 Ω	1%
R3	1000 Ω	1%
R4	47 Ω	1%
C1	1nF	5%
C2	10nF	5%
Vb	47V*	2%
RL	6.8 Ω	1%
LL	4.5mH	5%
Temp	25°C	-40°C and 105°C

Table 1.

*For the Zener voltage, that is the main parameter to be checked at this project, it is defined an extra voltage drift according to the temperature and following the component supplier datasheet of (0.05V/°C) taking 25°C as the initial point.

After calculation of the transient responses of given “N” outcomes, it is executed a code to get the clamping zone over the transient response and calculate an average value over all this range. Having the average Clamping voltage, it is performed a yield estimation using the code to evaluate the average clamping voltage versus the given limits (Refer to Appendix “3.-“). These limits are defined by a Worst Case Analysis in three temperatures: 25°C, -40°C and 105°C. The temperatures are chosen in order to fulfill the customer requirements of temperature operation of the circuit. In Figure 6 it is shown the MCA transient result of 500 outcomes at 25°C. The zoom over Clamping zone is shown at Figure 7.

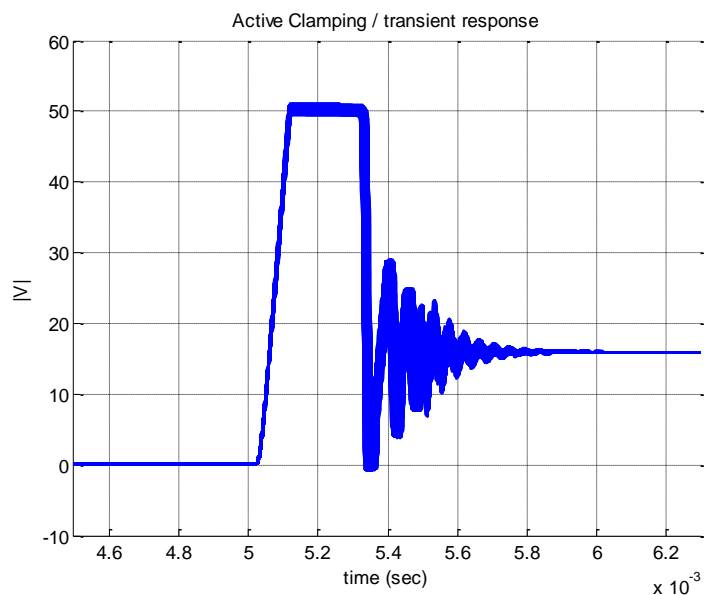


Figure 6.

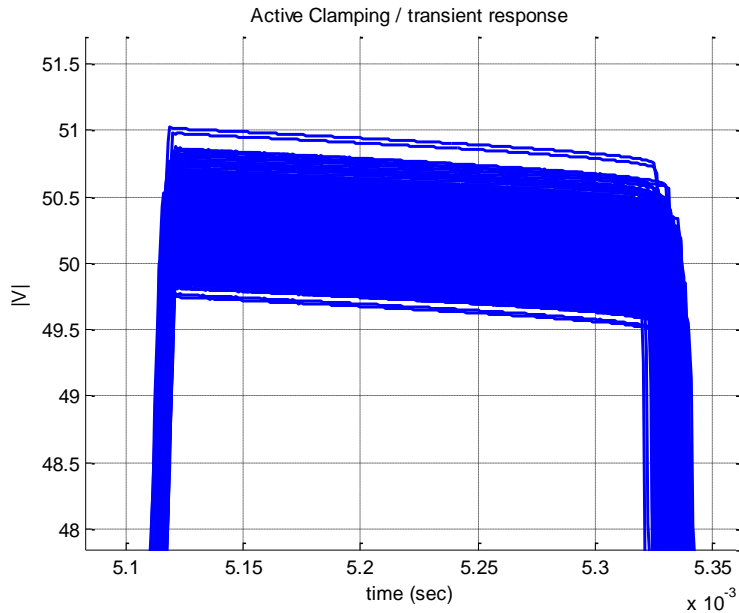


Figure 7.

In the Figure 8 it is shown the histogram for the 500 outcomes for the MCA in the active clamping voltage, showing the actual distribution of the clamping voltage readings.

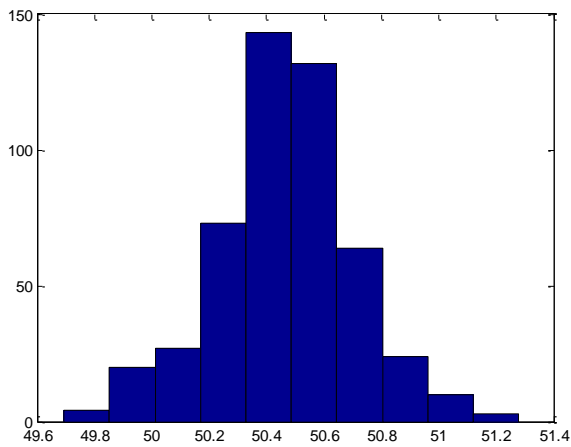


Figure 8.

```

Command Window
Active Clamping LSD
Temp=25
min_AVG=49.6943
max_AVG=51.2781
Upper limit=53.81
Lower limit=47.68
Yield Estimation
Yield =100 %
Outcomes =500
Press a key !
fx >> |
  
```

Figure 9.

The Yield is 100% as all the readings are within the limits given by the WCA. (See Figure 9). The MCA result for other temperatures are shown in Appendix "4.-" for -40°C and "5.-" for 105°C.

CONCLUSIONS

After being running the Monte Carlo Analysis with a Yield result of 100% at the three temperatures can tell us that the limits provided by the WCA are correct. With the histogram shown at Figure 8 it is checked that the readings are centered among the limits at 25°C, so the test is stable and the dispersion is not significant. We have to state that the limits for 25°C are tightened in order to catch zener diodes with a bad Break voltage as at this temperature it is easy to set the limits as all the parameters characterization of the zener are reported at 25°C in the datasheet.

This project helps to prove that some combination in the tolerances of the components could not cause a Clamping voltage reading to be out of the limits provided by the WCA being a good reading. The WCA limits are done using extreme values for the tolerances of the components, not taking in consideration all the possible combinations and thus the worst case for the Clamping Voltage. It is very difficult to have analytical exact limits that consider all the possible combinations of tolerances that create the worst scenario in a circuit. The circuits are getting complex and have multiple variables hard to track as the temperature in a silicon device.

I had problems to find a compatible Spice model for the initial MOSFET I chose as its model was so complex and did not run when I was trying to adapt it to WINSPICE. Then I chose one FET that has a simpler spice model that works well at WINSPICE. I think the chosen model is no so accurate representing the MOSFET at different temperatures, but it is good for the purposes of this project.

With the results of this project I have a better panorama of the behavior of the circuit among all the temperatures and if the limits calculated in the WCA could catch a bad component in a functional test.

BIBLIOGRAPHY

- MATLAB™, The MathWorks Inc., Natick, MA, 2010.
- WINSPIICE[©] Version: 1.04.02
- <http://desi.iteso.mx/erayas/cad.htm>
- “Estimating MOSFET Parameters from the Data Sheet”
<http://www.ti.com/lit/ml/slup170/slup170.pdf>

APENDIX

1.- Active Clamping circuit described in Spice and mounted in a Matlab function

```
%José Antonio Rodríguez Castañeda md193781
%Matlab driver for WinSpice Active Clamping Circuit for LSD Power Output
function [time ,R] = Active_Clamping(x)

%Define SPICE Script, ss

ss{1} = 'Active Clamping over a LowSide Driver power stage';
ss{2} = '* -----';
ss{3} = '* A.Rodriguez Final Project. ';
ss{4} = '* -----';
ss{5} = '* ';
ss{6} = 'Vsys VBATT 0 DC 16';
ss{7} = '*Load declaration';
ss{8} = ['LL VBATT 1 ' num2str(x(9)) 'mH'];
ss{9} = ['RL 1 2 ' num2str(x(5))];
ss{10} = ' *LSD declaration';
ss{11} = ['C1 3 5 ' num2str(x(6)) 'nF'];
ss{12} = ['C2 2 0 ' num2str(x(7)) 'nF'];
ss{13} = 'D1 8 2 BZX84C51/ZTX';
ss{14} = 'D2 8 4 BAT64/SIE';
ss{15} = ['R1 4 5 ' num2str(x(1))];
ss{16} = ['R2 5 0 ' num2str(x(2))];
ss{17} = ['R3 5 6 ' num2str(x(3))];
ss{18} = ['R4 3 2 ' num2str(x(4))];
ss{19} = 'XF 2 5 0 nvmfd5485nltlg';
ss{20} = '*Pre-driver simplification';
ss{21} = 'IGD1 VBATT 6 DC 0A PULSE (0A 14mA 0s 1ns 1ns 5ms 500ms)';
ss{22} = 'IGD2 6 0 DC 0A PULSE (0A 14mA 5.5ms 1ns 1ns 5ms 500ms)';
ss{23} = '* ZETEX BZX84C51 Spice Model Last Revision 1/10/96';
ss{24} = '*';
ss{25} = '.MODEL BZX84C51/ZTX D IS=228.7E-15 N=1.22 RS=.11 KF=1 XTI=3
EG=1.11';
ss{26} = ['+ CJO=21.92E-12 M=.3415 VJ=.7656 FC=.5 BV= '
num2str(x(8))];
ss{27} = ['+ IBV=.1079 TT=274.1E-9 TNOM= ' num2str(x(10))];
ss{28} = '*';
ss{29} = '* For later versions of Spice use the following parameter to
obtain';
ss{30} = '* better zener voltage variation over temperature.';
ss{31} = '* TBV1=.99E-3';
ss{32} = '*';
ss{33} = '*****';
ss{34} = '.MODEL BAT64/SIE D(';
ss{35} = '+ AF= 1.00E+00 BV= 3.00E+01 CJO= 6.59E-12 EG=
1.11E+00';
ss{36} = '+ FC= 5.00E-01 IBV= 1.00E-04 IS= 6.97E-09 KF=
0.00E+00';
ss{37} = '+ M= 3.96E-01 N= 1.01E+00 RS= 1.84E+00 TT= 1.00E-
10';
ss{38} = '+ VJ= 3.42E-01 XTI= 3.00E+00)';
ss{39} = '.SUBCKT nvmfd5485nltlg 1 2 3';
ss{40} = '*****';
```

```

ss{41} = '*      Model Generated by MODPEX      *';
ss{42} = '*Copyright(c) Symmetry Design Systems*';
ss{43} = '*      All Rights Reserved      *';
ss{44} = '*      UNPUBLISHED LICENSED SOFTWARE *';
ss{45} = '*      Contains Proprietary Information *';
ss{46} = '*      Which is The Property of      *';
ss{47} = '*      SYMMETRY OR ITS LICENSORS      *';
ss{48} = '*Commercial Use or Resale Restricted *';
ss{49} = '*      by Symmetry License Agreement *';
ss{50} = '*****';
ss{51} = '* Model generated on Jul 31, 13';
ss{52} = '* MODEL FORMAT: SPICE3';
ss{53} = '* Symmetry POWER MOS Model (Version 1.0)';
ss{54} = '* External Node Designations';
ss{55} = '* Node 1 -> Drain';
ss{56} = '* Node 2 -> Gate';
ss{57} = '* Node 3 -> Source';
ss{58} = 'M1 9 7 8 8 MM L=100u W=100u';
ss{59} = '* Default values used in MM:';
ss{60} = '* The voltage-dependent capacitances are';
ss{61} = '* not included. Other default values are:';
ss{62} = '*   RS=0 RD=0 LD=0 CBD=0 CBS=0 CGBO=0';
ss{63} = '.MODEL MM NMOS LEVEL=1 IS=1e-32';
ss{64} = '+VTO=2.68841 LAMBDA=0 KP=76.5747';
ss{65} = '+CGSO=4.95684e-06 CGDO=1e-11';
ss{66} = 'RS 8 3 0.0207068';
ss{67} = 'D1 3 1 MD';
ss{68} = '.MODEL MD D IS=1.18893e-11 RS=0.0041311 N=1.07679 BV=68';
ss{69} = '+IBV=0.00025 EG=1 XTI=2.39558 TT=0';
ss{70} = '+CJO=1.95548e-09 VJ=0.708387 M=0.9 FC=0.5';
ss{71} = 'RDS 3 1 1e+09';
ss{72} = 'RD 9 1 0.0111061';
ss{73} = 'RG 2 7 12';
ss{74} = 'D2 4 5 MD1';
ss{75} = '* Default values used in MD1:';
ss{76} = '*   RS=0 EG=1.11 XTI=3.0 TT=0';
ss{77} = '*   BV=infinite IBV=1mA';
ss{78} = '.MODEL MD1 D IS=1e-32 N=50';
ss{79} = '+CJO=6.81119e-10 VJ=1.5551 M=0.9 FC=1e-08';
ss{80} = 'D3 0 5 MD2';
ss{81} = '* Default values used in MD2:';
ss{82} = '*   EG=1.11 XTI=3.0 TT=0 CJO=0';
ss{83} = '*   BV=infinite IBV=1mA';
ss{84} = '.MODEL MD2 D IS=1e-10 N=0.4 RS=3.00001e-06';
ss{85} = 'RL 5 10 1';
ss{86} = 'FI2 7 9 VFI2 -1';
ss{87} = 'VFI2 4 0 0';
ss{88} = 'EV16 10 0 9 7 1';
ss{89} = 'CAP 11 10 9.74541e-10';
ss{90} = 'FI1 7 9 VFI1 -1';
ss{91} = 'VFI1 11 6 0';
ss{92} = 'RCAP 6 10 1';
ss{93} = 'D4 0 6 MD3';
ss{94} = '* Default values used in MD3:';
ss{95} = '*   EG=1.11 XTI=3.0 TT=0 CJO=0';

```

```

ss{96} = '* RS=0 BV=infinite IBV=1mA';
ss{97} = '.MODEL MD3 D IS=1e-10 N=0.4';
ss{98} = '.ENDS nvdfd5485nlt1g';
ss{99} = '.control';
ss{100} = [' temperature = ' num2str(x(10))];
ss{101} = ' TRAN 0.001ms 7.5ms';
ss{102} = ' *plot mag(V(2))';
ss{103} = ' write Active_Clamping.csv V(2)';
ss{104} = 'quit';
ss{105} = '.endc';
ss{106} = '.end';

%Save SPICE Script as a Circuit File in Matlab Working Directory
CircuitFileName = 'Active_Clamping.cir';
ckt_file = char (ss); %Conver cell array "ss" ti character Array
[rows,~] = size (ckt_file); %Read number of rows in "ckt_file".
fid = fopen(CircuitFileName,'w+');%File identified opened.
for i = 1:rows %Save each row of character array
    fprintf(fid, '%s',ckt_file(i,:));%"ckt_file" in ASCII file
    fprintf(fid, '%s\r\n', ''); %Circuit file name
end

fclose(fid); %File identifier closed.

%Run Winspice Circuit File

ExecFile= 'C:\WINSPICE\PF_ARC\wspice3 ';
system([ExecFile CircuitFileName]);

%Read WinspiceOutput Files
Active_C_file = csvread('Active_Clamping.csv',1,0); %Read transient responses
time = Active_C_file(:,1);
R = Active_C_file(:,2);

%Erase WinSpice Output Files
delete Active_Clamping.csv;

end

```

2.- MCA code in matlab for the Active Clamping

```

%José Antonio Rodríguez Castañeda md193781
%Monte-Carlo Analysis for Active Clamping Circuit for LSD Power Output

```

```

%Nominal Design
Temp=25; %Temperature in °C
R1=100; %Resistor Values (Ohms)
R2=4700; %Resistor Values (Ohms)
R3=1000; %Resistor Values (Ohms)
R4=47; %Resistor Values (Ohms)
RL=6.8; %Resistor Values (Ohms)

```

```

C1=1;      %Capacitor Value (nF).
C2=10;    %Capacitor Value (nF).
if Temp==25 %Zener BreakDown Voltage
Vb=47;
elseif Temp==105
Vb=47+4; %105°C (0.05V/°C)
else % -40°C (0.05V/°C)
Vb=47-3.25;
end
LL=4.5;   %Inductor Value (mH).

Ynom = [R1 R2 R3 R4 RL C1 C2 Vb LL Temp]; % Selected parameters vector.

%Calculate Clamping result at nominal Design
[time_nom ,R_nom] = Active_Clamping(Ynom);

%Define OutComes and Tolerances
N=500;
tauR1=0.05; %Tolerance for R1
tauR2=0.01; %Tolerance for R2
tauR3=0.01; %Tolerance for R3
tauR4=0.01; %Tolerance for R4
tauRL=0.01; %Tolerance for RL
tauC1=0.05; %Tolerance for C1
tauC2=0.05; %Tolerance for C2
tauVb=0.02; %Tolerance for Vb
tauLL=0.05; %Tolerance for LL
tauTemp=0.08; %Tolerance for Temp

tau= [tauR1 tauR2 tauR3 tauR4 tauRL tauC1 tauC2 tauVb tauLL tauTemp];

%Generate Random OutComes with Gaussian (Normal) PDF
Y = zeros(N,length(Ynom));
for j = 1:N
    Y(j,1)=Ynom(1)*(1+tau(1)*(2*(0.5+0.13*randn)-1));
    Y(j,2)=Ynom(2)*(1+tau(2)*(2*(0.5+0.13*randn)-1));
    Y(j,3)=Ynom(3)*(1+tau(3)*(2*(0.5+0.13*randn)-1));
    Y(j,4)=Ynom(4)*(1+tau(4)*(2*(0.5+0.13*randn)-1));
    Y(j,5)=Ynom(5)*(1+tau(5)*(2*(0.5+0.13*randn)-1));
    Y(j,6)=Ynom(6)*(1+tau(6)*(2*(0.5+0.13*randn)-1));
    Y(j,7)=Ynom(7)*(1+tau(7)*(2*(0.5+0.13*randn)-1));
    Y(j,8)=Ynom(8)*(1+tau(8)*(2*(0.5+0.13*randn)-1));
    Y(j,9)=Ynom(9)*(1+tau(9)*(2*(0.5+0.13*randn)-1));
    Y(j,10)=Ynom(10)*(1+tau(10)*(2*(0.5+0.13*randn)-1));
end

%Calculate Responses of Interest at Random OutComes
tl=7500; %Fixed analysis time
Resp = zeros(N,tl);
for j = 1:N
    [time,R]= Active_Clamping(Y(j,:));

```

```

Resp(j,:)=R(1:t1);
hold on;
plot(time(4500:6500),R(4500:6500),'b-','LineWidth',1.5);
xlim([0.0045 0.0063])
title('Active Clamping / transient response')
xlabel('time (sec)');
ylabel('|V|');
grid on
end

AVG_buffer=zeros(1,N);
for o=1:N
    %Get Clamping zone
    CZStart=0; %Start point
    CZSflag=0; %Start Flag
    CZEnd=0; %End point
    CZEflag=1; %End flag
    for j=4500:6500
        if Resp(o,j)>40
            %Start Point
            if CZSflag==0
                if (Resp(o,(j-1))-Resp(o,j))>0
                    CZStart=j+1; %Safety_Zone
                    CZSflag=1;
                    CZEflag=0; %Set End point serching flag
                end
            end
        end

        %End Point
        if CZEflag==0
            if (Resp(o,(j-1))-Resp(o,j))>0.5
                CZEnd=j-4; %Safety zone
                CZSflag=1;
                CZEflag=1; %Points have been obtained
            end
        end
    end
end
end

%k=CZEnd-CZStart; %Measurement window
for k=CZStart:CZEnd
    AVG_buffer(o)= AVG_buffer(o) + Resp(o,k);
end
AVG_buffer(o)= AVG_buffer(o) / (CZEnd-CZStart);

end

clc;
disp('Active Clamplng LSD')
disp(['Temp=' num2str(Temp)]);
disp(['min_AVG=' num2str(min(AVG_buffer))]);
disp(['max_AVG=' num2str(max(AVG_buffer))]);

%Yield Analysis

```

```

u=zeros(1,N);
Ia=ones(1,N);
Disp_flag=1;
for j = 1:N
    u(j)=MinMax_AC(AVG_buffer(j),Temp,Disp_flag);
    if u(j) > 0
        Ia(j)=0;
    end
    Disp_flag=0;
end

yield=sum(Ia)/N;
disp('Yield Estimation')
Yield_label = ['Yield = ' num2str(yield*100) ' %'];
disp(Yield_label);
disp(['Outcomes = ' num2str(N)]);

disp('Press a key !') % Press a key here.
pause;
close all;

hist(AVG_buffer);

```

3.- Min Max evaluation for Yield estimation

```

%José Antonio Rodríguez Castañeda md193781
%Yield estimation for Active Clamping Circuit

```

```

function u=MinMax_AC(AVG_buffer,Temp,flag)
%Design Specs
if Temp==25
AVG_UB=53.81;
AVG_LB=47.68;
elseif Temp==105
AVG_UB=56.46;
AVG_LB=49.23;
else
AVG_UB=50.08;
AVG_LB=45.08;
end

if flag==1
disp(['Upper limit=' num2str(AVG_UB)]);
disp(['Lower limit=' num2str(AVG_LB)]);
end
%Evaluate Vector of Error Functions
eps=1e-12;
e1 = AVG_buffer / (AVG_UB+eps) -1;
e2 = 1 - AVG_buffer/(AVG_LB+eps);
e=[e1 e2];

u = max(e);

```

end

4.- MCA result at -40°C

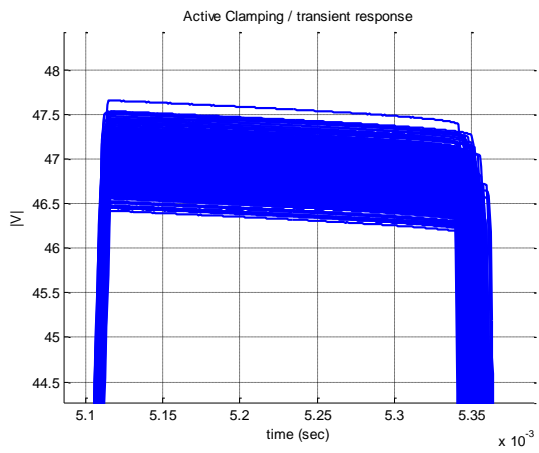
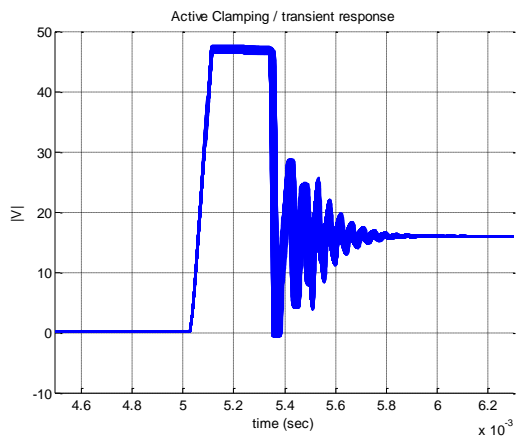
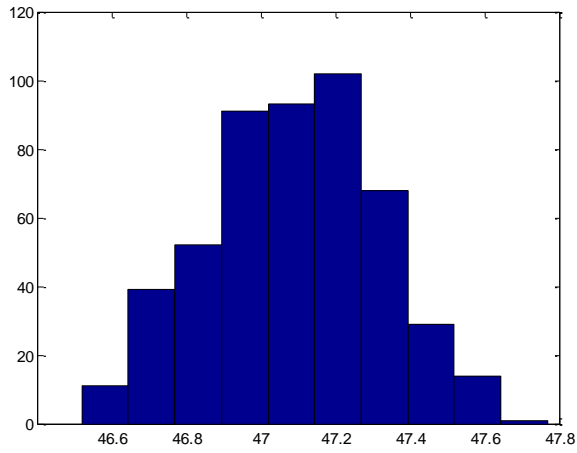


Figure 10.

Figure 11.



Command Window

```

Active Clamplng LSD
Temp=-40
min_AVG=46.4128
max_AVG=47.932
Upper limit=50.08
Lower limit=45.08
Yield Estimation
Yield =100 %
Outcomes =500
Press a key !

```

f_x >>

Figure 12.

Figure 13.

5.- MCA result at 105°C

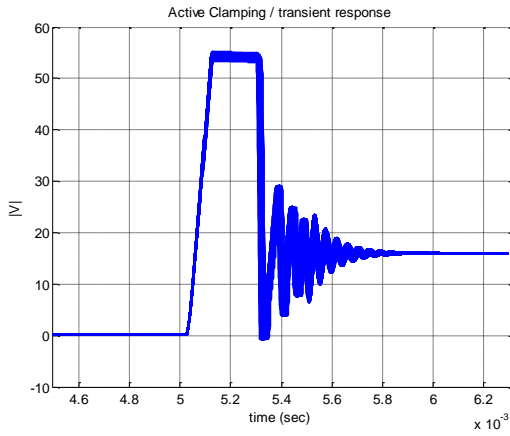


Figure 14.

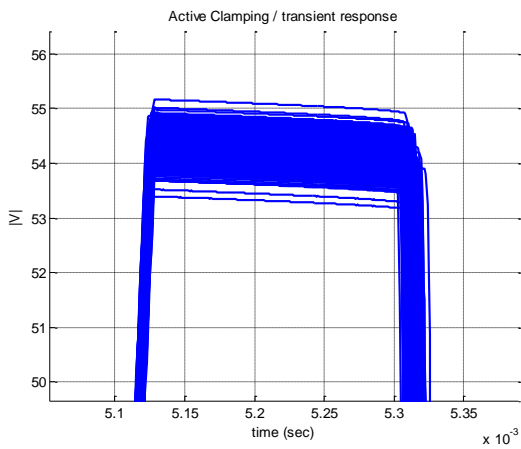


Figure 15.

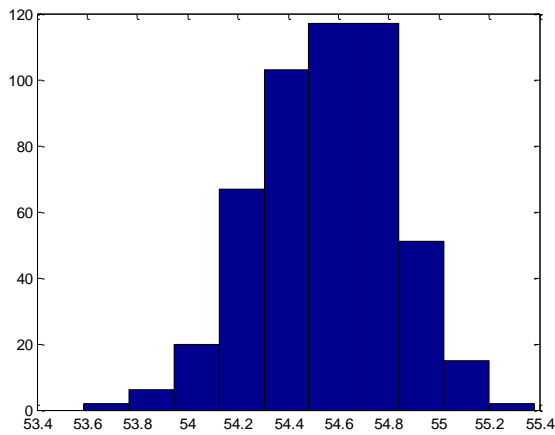


Figure 16.

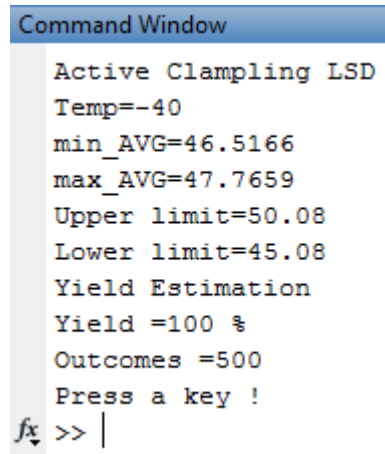


Figure 17.

C. ON TIME AND POWER OPTIMIZATION OF AN ACTIVE CLAMPING CIRCUIT IN A LOW SIDE DRIVER POWER OUTPUT

INTRODUCTION

The intention of this project is to implement an Optimization Algorithm with the Active Clamping Circuit in order to fulfill a given requirements. This circuit is used in a Low Side Driver (LSD) Power Output to accelerate the current decay of an inductive-resistive valve. In general the LSD creates a path to ground for the load when it is active and can be toggled at different Frequencies and Pulse Width Modulation in order to get the desired current at the load.

Power outputs are used in automotive in order to control valves such as the Fuel Pump or the Starter of the engine. It are some specific requirements of discharge time of the load, or in other words, the “ON time” of the active clamping circuit. Having a lower discharge time can increase the frequency of toggling the load and also it is a matter of safety if the load is related to torque in the vehicle.

When trying to reduce the discharge time, it is very important to take care of the total amount of energy dissipated over the FET, as in this active clamping circuit the current of the load is discharged over the FET. A brief explanation of the LSD operation is reported in the Theory section in order to give to the reader the basic knowledge about this Power Output and the expected response over the transient response.

The purpose of this project is to find the components that satisfy the discharge time requirements of the customer and at the same time have a power dissipative below the design requirements so the designer can choose properly the FET to be used.

It is very important to fulfill the discharge time requirements, so the valve can be closed or discharged as requested. Also it is very important to be sure the FET is capable of handling the power dissipation of the discharge.

Theory

The Low Side Driver is a circuit that provides a path to Ground to a specific load. It uses a N-channel MOS with source connected to ground. The basic schematic for a LSD is shown at Figure 1.

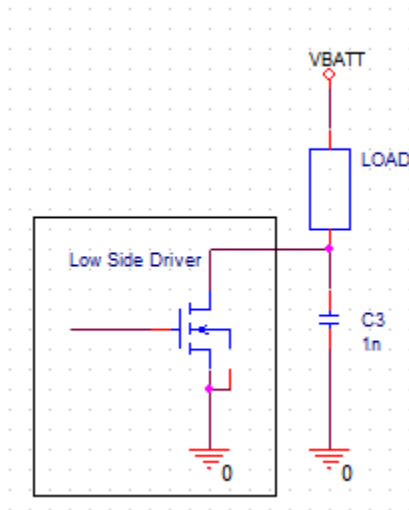


Figure 1.

Different Loads can be used with a LSD in order to control the current flowing to ground switching the Mosfet. Examples of these loads are relays, valves, solenoids and heaters. The circuitry to be analyzed at this project is shown at Figure 2.

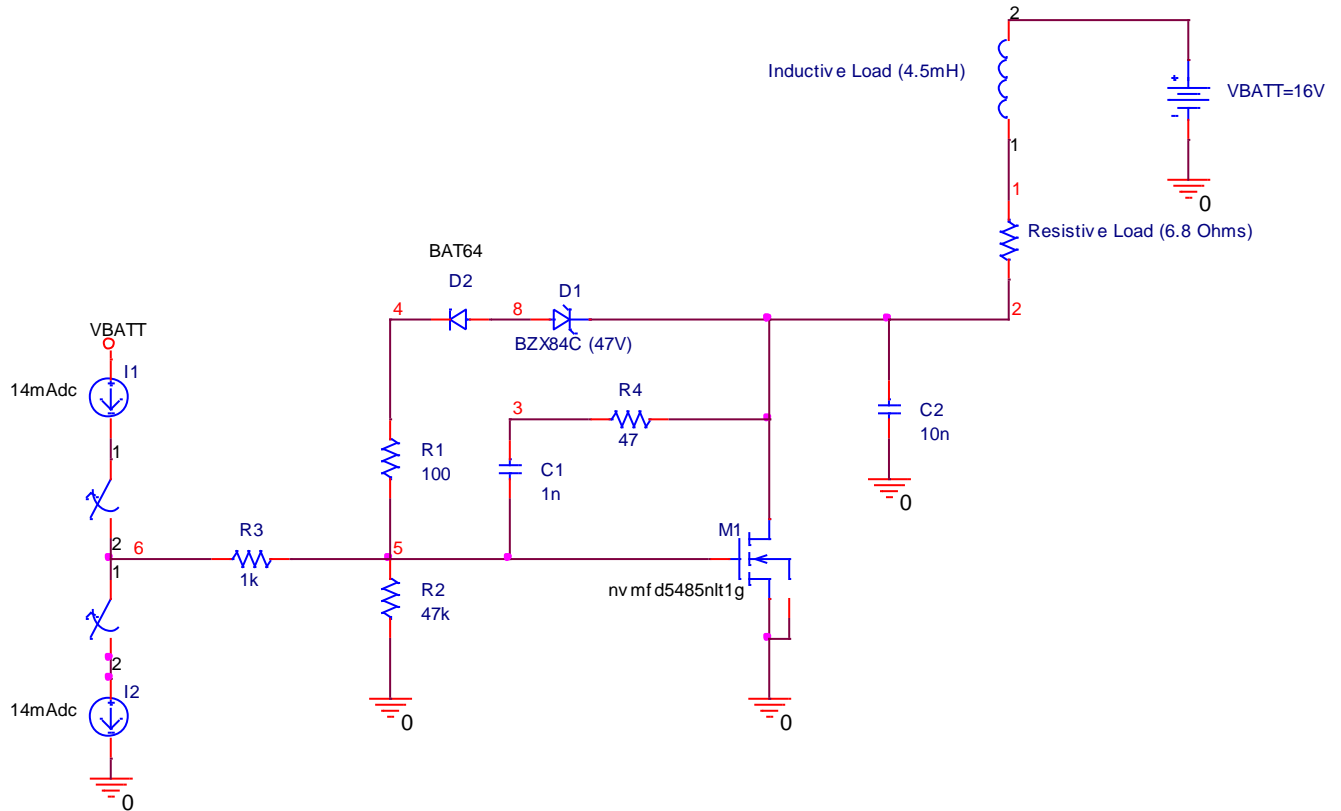


Figure 2.

This is the explanation of how the circuit works: M1 Mosfet is used to create the path to ground for the load, so when it is turned ON the current start to increase and takes some time in order to reach the maximum current given by the resistive part of the load if the duty cycle of the ASIC driver allows it.

$$I_{max} = \frac{V_{batt}}{R(load)} \quad Eq1.$$

The mosfet is activated by a pre-driver (ASIC) that handles the activation profile and another functionalities as the diagnostic of the power stage (not represented in Figure 2). The ASIC is represented with the two current sources, I1 and I2, that allows the pre-driver to turn ON or OFF the FET.

When the FET is ON, the current is flowing through the load and energy is stored in the inductor as magnetic field. When the FET is turned OFF, the inductor starts increasing its voltage in order to find a way to discharge all this energy. The inductor finally finds a way to discharge a little current breaking the Vb of the Zener D1 and flowing to ground through R1, R2 and the gate of the M1 (See Figure 3).

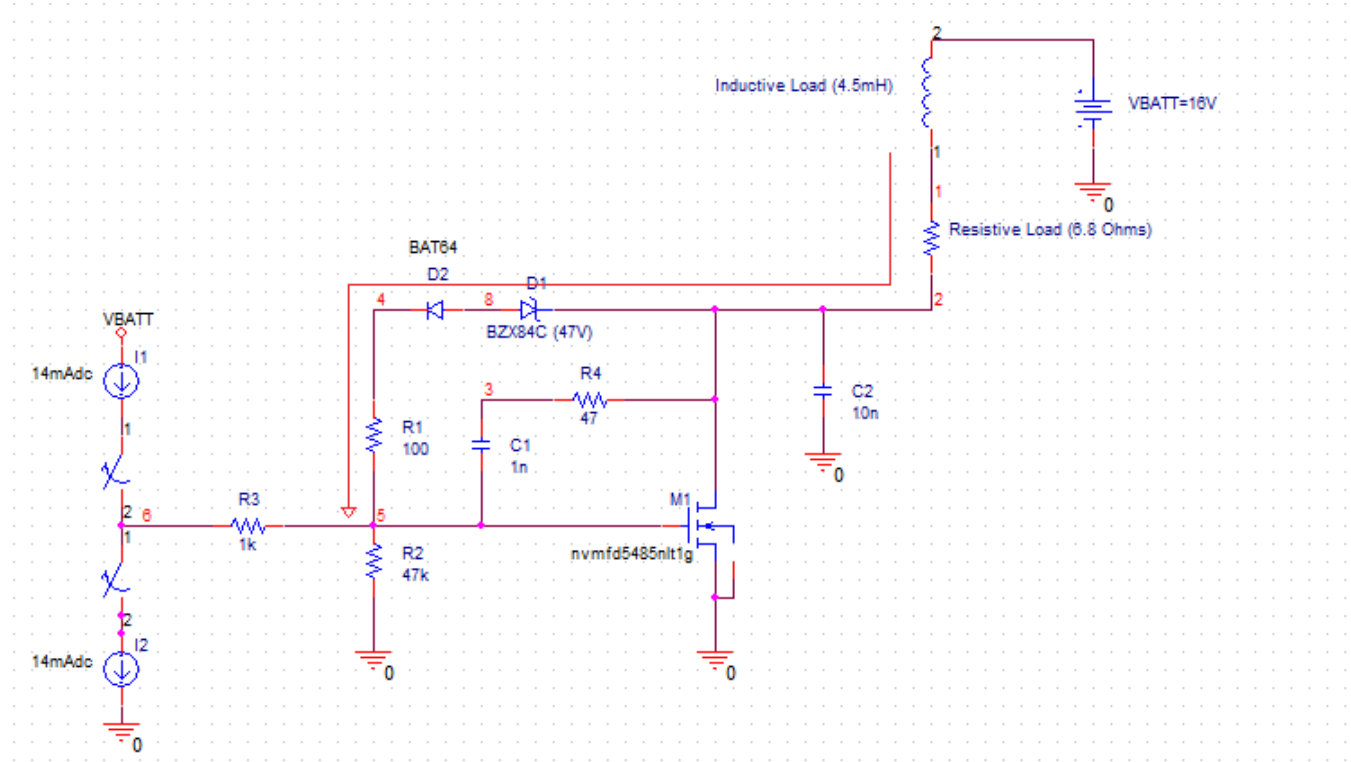


Figure 3.

At the same time the branch across the Zener D1 will activate the FET M1 and starting discharging a little bit the inductor through the M1 drain to ground. But this will decrease the inductor voltage below the VB of D1, cutting off the branch described and turning the FET M1 OFF. With the FET in OFF state the inductor will start to increase its voltage again to reach the VB of D1 threshold. The circuit will be playing turning ON and OFF the FET moving the inductor voltage and at the same time discharging the energy. This is called “Active Clamping”.

This cycle will be repeated in a control closed loop, with the M1 FET playing in the non-linear zone (Ohmic region) and discharging the inductor across the M1 drain and setting a voltage at node 2 given by the following:

$$V(2) = Vz + Vf + V(R1) + V_{plateau}(M1) \tag{Eq.2}$$

Where:

- Vz=Vbreak voltage of the Zener D1
- Vf=Forward voltage of D2
- V(R1)=Voltage droop over R1
- Vplateu(M1)= Plateu voltage of M1

The plateau voltage is the VGS voltage when the FET starts to conducting and entering into the Ohmic Region. In Figure 4 the plateau voltage is the flat area of VGS vs the Gate Charge.

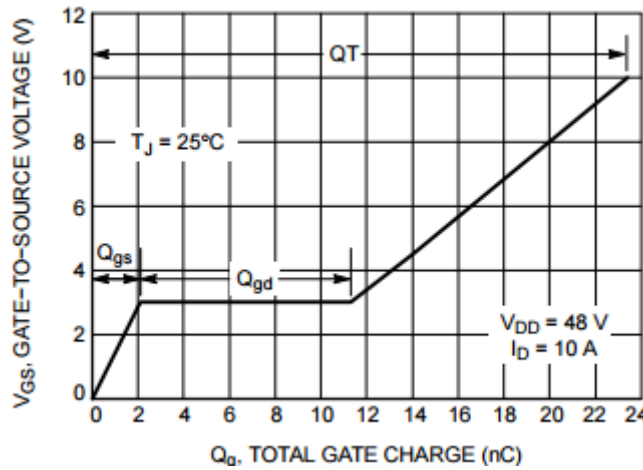


Figure 4.

The plateau voltage is dependent of the construction process of the mosfet and will vary from each silicon wafer to another. A good approximation taken from design team is $2.4 < V_{plateu} < 3.4$. A good way to estimate this value from a given mosfet is explained in this documente from TI: “Estimating MOSFET Parameters from the Data Sheet”. Web page link stated in the Bibliography.

So taking Vz=47v, Vf=0.6v, Vplateu=3v :

$$V(R1) = \frac{V_{plateu}}{R2 || R3} * R1 = 306mV$$

$$V(2) = 47 + 0.6 + 0.306 + 3 = 50.906V$$

This V(2)=50.906V is the nominal response for the Active Clamping Voltage at 25°C.

The discharge time of the current in the load will depend of the Active Clamping Voltage and the slew rate circuitry at the FET’s gate. As this circuit is a control loop design, it is a little difficult to get an exact mathematical equation to represent the response of the whole circuit.

Experiment

The circuit of Figure 2 was implemented in a SPICE file and mounted over a Matlab driver function in order to receive specific parameters, run the with WINSPIICE, save the result in a*csv file and return the transient analysis to the call function. Please refer to Appendix “1.-“.

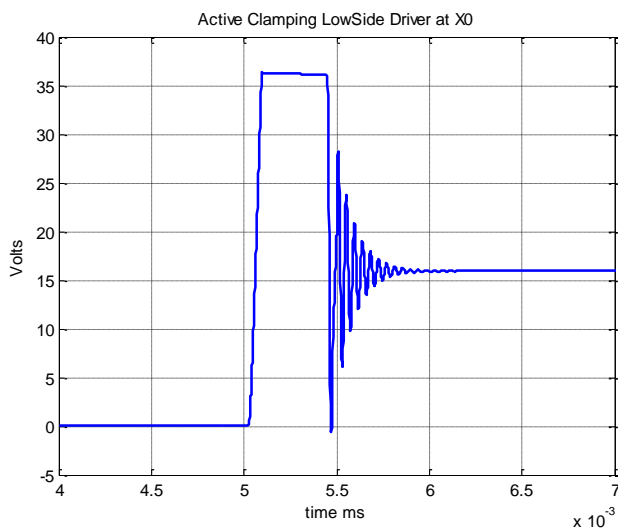
In the previous course it was implemented a Monte Carlo Analysis over this circuit. Check the Final Project report for further information about the Active Clamping Circuit and the corroboration that the circuit SPICE model was working as expected.

1. Optimization Variables and Starting Point

The selected vector of optimization variables is $x=[V_b(V) \ R4(\Omega) \ C2(nF)]^T$

The first starting point for optimization is $x_0=[33 \ 47 \ 1]^T$

Circuit response at x_0 :



Power (mW) at initial Point

$P = 12.103717469703588$

On time (us) at initial Point

$OT = 3.540000000000470e+002$

Figure 5.

2. Design Specifications

Let ,

P =Power during the Active Clamping

OT = ON time of the Active Clamping

Design specs during Active Clamping zone are:

$$P < 7.5mW = s_2^{UB}$$

$$OT < 150us = s_1^{UB}$$

3. Formulation of the Optimization Problem

$$x^* = \arg \min_x \max \{ \dots e_k(x) \dots \}$$

Where the k-th error function is given by

$$e(x) = \begin{cases} \frac{OT}{s_1^{UB} + \varepsilon_1} - 1 \\ \frac{P}{s_2^{UB} + \varepsilon_2} - 1 \end{cases}$$

With $\varepsilon_1 = \frac{s_1^{UB}}{100}$ and $\varepsilon_2 = \frac{s_2^{UB}}{100}$

As the variables to be optimized need to be within some physical limits, the Optimization Problem can be represented as following to implement box constraints:

$$z^* = \arg \min_z \max \{ \dots e_k(z) \dots \}$$

Where the k-th error function is given by

$$e(z) = \begin{cases} \frac{OT}{s_1^{UB} + \varepsilon_1} - 1 \\ \frac{P}{s_2^{UB} + \varepsilon_2} - 1 \end{cases}$$

With $\varepsilon_1 = \frac{s_1^{UB}}{100}$ and $\varepsilon_2 = \frac{s_2^{UB}}{100}$

and $\mathbf{x} = \begin{bmatrix} x_1 \\ x_2 \\ x_3 \end{bmatrix} = \begin{bmatrix} x_1^{lb} + (x_1^{ub} - x_1^{lb})(\sin z_1)^2 \\ x_2^{lb} + (x_2^{ub} - x_2^{lb})(\sin z_2)^2 \\ x_3^{lb} + (x_3^{ub} - x_3^{lb})(\sin z_3)^2 \end{bmatrix}$ with $\mathbf{x}^{lb} = [32 \quad 20 \quad 1]$ $\mathbf{x}^{ul} = [55 \quad 60 \quad 10]$

4. Objective Function Implementation

```
%José Antonio Rodríguez Castañeda    mdl93781
%Optimization-Based Modeling and Design of Electronic Circuits
%Usage: [R,fl]=OF_OA_AC(X)
% X = [Vb R4 C1]', design variables.
% e_max : Maximum error against optimization requirements
% Objective Function for Active Clamping for a LowSide Driver circuit
function [e_max] = OF_OA_AC(x)

%Box Constraints (Create xi from zi)
%Vb
Vb_LB=32;
Vb_UB=55;
Vbi=Vb_LB+(Vb_UB-Vb_LB)*(sind(x(1))^2);
%R4
R4_LB=20;
R4_UB=60;
R4i=R4_LB+(R4_UB-R4_LB)*(sind(x(2))^2);
%C2
C2_LB=1;
C2_UB=10;
C2i=C2_LB+(C2_UB-C2_LB)*(sind(x(3))^2);
```

```

%Error limits
Ti_UB=150; %Discharge time requirement
Po_UB=7.5; %Max power requirement mW
Delta_t=Ti_UB/100; %Time Delta
Delta_p=Po_UB/100; %Power Delta

xp=[Vbi R4i C2i]; %Create xi inputs

%Get actual response with xi
[time,R,Cur] = AC(xp);

[P,OT]=Power_Time(R,time,Cur); %Calculate On Time and Power dissipation

%Calculate actual error

e1n= (OT)/(Ti_UB+Delta_t) -1; %On_time error
e2n=(P)/(Po_UB+Delta_p) -1; %Power error

e=[e1n e2n];
e_max=sum(abs(e)); %Create maximum error

end

```

5. Optimization Algorithm

It was chosen the Nelder-Mead method to find the solution. The matlab code is shown below:

```

%José Antonio Rodríguez Castañeda md193781
%Optimization-Based Modeling and Design of Electronic Circuits
%Active Clamping optimization algorithm for a LowSide Driver circuit
%Nelder-Mead Optimization Algorithm
% Fminsearch Test for Active Clamping

display('*****Active Clamping ON Time and Power Optimization Algorithm
*****')
display(' ')

% Fminsearch input arguments
MaxIter=70;
epsf=0.1;
epsx=0.1;

%Output argument
Iter=0;
FunEval=0;
EF=0;

%FminSearch Options

```

```

options=optimset('Display','off','FunValCheck','off','MaxFunEvals',(MaxIter*1
0),'MaxIter',MaxIter,'OutputFcn',[],'PlotFcns',[],'TolFun',[epsf],'TolX',[eps
x]);

%-----Starting Points-----
display('***** Starting point *****')
x0_1(1)=33; %Vb Volts
x0_1(2)=47; %R4 Ohms
x0_1(3)=1; %C2 nF

x0_2(1)=49; %Vb Volts
x0_2(2)=10; %R4 Ohms
x0_2(3)=5; %C2 nF

x0_3(1)=40; %Vb Volts
x0_3(2)=59; %R4 Ohms
x0_3(3)=2; %C2 nF

x0=x0_1

%Select Driver function to display initial waveform
fun1=@AC;
%Plot initial response
[t,R,Cur] = fun1(x0);
plot(t,R, 'b','LineWidth',2);
[P,OT]=Power_Time(R,t,Cur);
grid on;
hold on;
xlim([4e-3 7e-3])
%title('Active Clamping LowSide Driver at X0');
title('Active Clamping LowSide Driver');
xlabel('time ms')
ylabel('Volts')
%Display initial Power and ON Time
display('Power (mW) at initial Point')
P
display('On time (us) at initial Point')
OT

%Select Objective Function for optimization
fun=@OF_OA_AC;
%Execute Optimization
[x,fval,EF,output]=fminsearch(fun,x0,options);
display('Solution found')

%Revert variables of the box constraint
%Vb
Vb_LB=32;
Vb_UB=55;
Vbi=Vb_LB+(Vb_UB-Vb_LB)*(sin(x(1))^2);
%R4
R4_LB=20;
R4_UB=60;

```

```

R4i=R4_LB+(R4_UB-R4_LB)*(sin(x(2))^2);
%C2
C2_LB=1;
C2_UB=10;
C2i=C2_LB+(C2_UB-C2_LB)*(sin(x(3))^2);

%Optimized Variables
xp=[Vbi R4i C2i]

%Display Solution circuit response
[t,R,Cur] = fun1(xp);
plot(t,R, 'r--', 'LineWidth',2);
%Display Solution ON Time and Power
[P,OT]=Power_Time(R,t,Cur);
display('Power (mW) at solution')
P
display('On time (us) at solution')
OT
display('Function Value at the solution')
fval
display('Number of iterations')
output.iterations
display('Number of Function Evaluations')
output.funcCount
display('Exit Flag')
EF
if EF==1
    display('fminsearch converged to a solution x.')
elseif EF==-1
    display('Maximum number of function evaluations or iterations was
reached')
else
    display('mAlgorithm was terminated by the output function. ')
end

```

6. Optimization Results

Using the starting point $x_0 = [33 \ 47 \ 1]$

The solution is shown at Figure 6. (On Blue the response at the starting point and on Red the response of the solution)

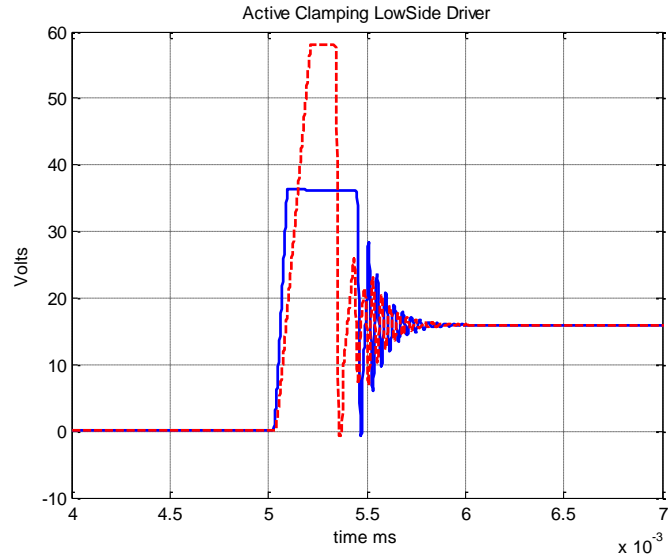


Figure 6.

The matlab script output text is shown below:

Solution found

xp =

54.901202315038944 30.310647458113891 1.791347672038179

Power (mW) at solution

P = 4.487186589319220

On time (us) at solution

OT = 1.260000000000167e+002

Function Value at the solution

fval = 0.080070975656048

Number of iterations

ans = 54

Number of Function Evaluations

ans = 108

Exit Flag

EF = 1 fminsearch converged to a solution x.

The solution satisfies the problem requirements and has elements that can be easily approximated with real electronic components. For example: $x_r = [55 \ 30 \ 1.8]$

Using the starting point $x_0 = [49 \ 10 \ 5]$

The solution is shown at Figure 7. (On Blue the response at the starting point and on Red the response of the solution)

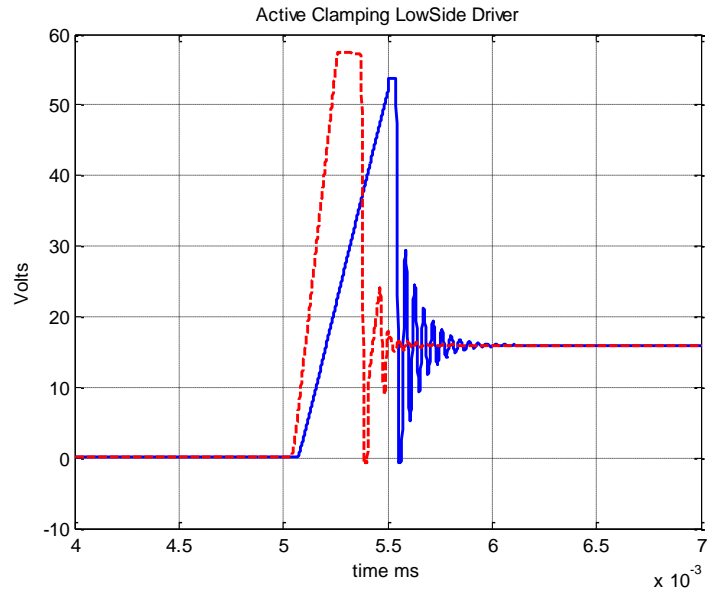


Figure 7.

The matlab script output text is shown below:

***** Starting point *****

x0 = 49 10 5

Power (mW) at initial Point

P = 0.360315674132811

On time (us) at initial Point

OT = 37.866701641793391

Solution found

xp = 54.196135251804023 57.541552297772689 2.251526213288758

Power (mW) at solution

P = 3.211312532712622

On time (us) at solution

OT = 1.090000000000153e+002

Function Value at the solution

fval = 0.063639201371567

Number of iterations

ans = 40

Number of Function Evaluations

ans = 85

Exit Flag

EF = 1 fminsearch converged to a solution x.

In this test case for the starting point $x_0 = [49 \ 10 \ 5]$ it are two remarkable statements to point out:

1.- The response using the starting point satisfies the problem requirements, but `fminsearch` continues iterating. The explanation is given by Matlab help tutorial 2* : “Unlike other solvers, `fminsearch` stops when it satisfies *both* `To1Fun` and `To1X..`”

2.- The objective function use the Manhattan Norm to calculate the error:

$$\textit{Manhattan Norm} = \sum_{i=1}^k |e_i(x)|$$

So the error is absolute, which means that as the result comes more negative (The general intention in an optimization problem) the absolute error value increase. This means that the solution only remains near to the limits.

This problem is taking advantage of this feature as it corrects the initial asymmetrical response and fits it into a more symmetrical response always fulfilling the problem requirements.

CONCLUSIONS

This project helps to optimize the design of an active clamping circuit in a Low Side Driver topology meeting customer requirements of discharge time and helping the designer to select the proper FET and its power rating. It was decided to use Nelder-Mead algorithm using a minmax formulation with box constraints and Manhattan Norm for the error calculation.

The results of the optimization satisfy the requirements of discharge time and power rating with the three starting points used in this experiment. Also it is remarkable that one starting point, that solution already fits the requirements, with a non-symmetrical response was corrected to a symmetrical response of the active clamping. The previous was due to the Manhattan Norm, which in this case creates the less error near to the limits because its calculation is based on the sum of the absolute errors.

The debug of the SPICE model for the active clamping circuit was done in the previous course “Simulation Methods for Electronic Circuits” when implementing a Monte Carlo Analysis. The above helped to reduce the time dedicated to implement the circuit in SPICE and the MATLAB driver development. Nevertheless it was difficult to obtain the ON Time and Power of the Current and Voltage waveforms doing it only with basic evaluations.

This optimization code could be very helpful to save design time when trying to fulfill changing requirements from customer and trying to implement a PCO (Product Cost Optimization) when selecting the proper FET with a lower power rating and therefore lower price. This circuit is commonly used in many outputs in the Electronic Control Units, so its optimization helps to the design team to save time and effort.

Another optimization experiment for this circuit could be to reduce the variation of the clamping voltage due to the components tolerance with an Optimization of the results of the Monte Carlo Analysis over temperature.

BIBLIOGRAPHY

1* -MATLAB™, The MathWorks Inc., Natick, MA, 2010.

2* - <https://www.mathworks.com/help/matlab/math/setting-options.html>

3* -WINSPICE[©] Version: 1.04.02

4* - <http://desi.iteso.mx/erayas/cad.htm>

5* - “Estimating MOSFET Parameters from the Data Sheet”

<http://www.ti.com/lit/ml/slup170/slup170.pdf>

APENDIX

1.- Active Clamping SPICE Driver and middle layer function

```
% Driving Active_Clamping.cir from Matlab
%
% José Antonio Rodríguez Castañeda md193781
% Optimization-Based Modeling and Design of Electronic Circuits
% This function drives the WINSPICE file Active_Clamping.cir from
% Matlab, and returns the simulation results in arrays time, R and Cur.
%
% Usage: [time,R, Cur] = AC_SPICE(X)
% X = [R1 R2 R3 R4 RL C1 C2 Vb LL Temp]', design variables and pre-assigned
% parameters
% time: Time array with the corresponding time points.
% R: Voltage magnitude response array
% Cur: Current magnitud response array
% Functions required: None.
function [time ,R,Cur] = AC_SPICE(x)

%Define SPICE Script, ss

ss{1} = 'Active Clamping over a LowSide Driver power stage';
ss{2} = '* -----';
ss{3} = '* A.Rodriguez Final Proyect. ';
ss{4} = '* -----';
ss{5} = '* ';
ss{6} = 'Vsys VBATT 0 DC 16';
ss{7} = '*Load declaration';
ss{8} = ['LL VBATT 1 ' num2str(x(9)) 'mH'];
ss{9} = ['RL 1 2 ' num2str(x(5))];
ss{10} = '*LSD declaration';
ss{11} = ['C1 3 5 ' num2str(x(6)) 'nF'];
ss{12} = ['C2 2 0 ' num2str(x(7)) 'nF'];
ss{13} = 'D1 8 2 BZX84C51/ZTX';
ss{14} = 'D2 8 4 BAT64/SIE';
ss{15} = ['R1 4 5 ' num2str(x(1))];
ss{16} = ['R2 5 0 ' num2str(x(2))];
ss{17} = ['R3 5 6 ' num2str(x(3))];
ss{18} = ['R4 3 2 ' num2str(x(4))];
ss{19} = 'XF 2 5 0 nvmfd5485nltlg';
ss{20} = '*Pre-driver simplification';
ss{21} = 'IGD1 VBATT 6 DC 0A PULSE (0A 14mA 0s 1ns 1ns 5ms 500ms)';
ss{22} = 'IGD2 6 0 DC 0A PULSE (0A 14mA 5.5ms 1ns 1ns 5ms 500ms)';
ss{23} = '* ZETEX BZX84C51 Spice Model Last Revision 1/10/96';
ss{24} = '*';
ss{25} = '.MODEL BZX84C51/ZTX D IS=228.7E-15 N=1.22 RS=.11 KF=1 XTI=3
EG=1.11';
ss{26} = ['+ CJO=21.92E-12 M=.3415 VJ=.7656 FC=.5 BV= '
num2str(x(8))];
ss{27} = ['+ IBV=.1079 TT=274.1E-9 TNOM= ' num2str(x(10))];
ss{28} = '*';
ss{29} = '* For later versions of Spice use the following parameter to
obtain';
ss{30} = '* better zener voltage variation over temperature.';
ss{31} = '* TBV1=.99E-3';
```

```

ss{32} = '*';
ss{33} = '*****';
ss{34} = '.MODEL BAT64/SIE D(';
ss{35} = '+      AF= 1.00E+00      BV= 3.00E+01      CJO= 6.59E-12      EG=
1.11E+00';
ss{36} = '+      FC= 5.00E-01      IBV= 1.00E-04      IS= 6.97E-09      KF=
0.00E+00';
ss{37} = '+      M= 3.96E-01      N= 1.01E+00      RS= 1.84E+00      TT= 1.00E-
10';
ss{38} = '+      VJ= 3.42E-01      XTI= 3.00E+00)';
ss{39} = '.SUBCKT nvbfd5485nltlg 1 2 3';
ss{40} = '*****';
ss{41} = '*      Model Generated by MODPEX      *';
ss{42} = '*Copyright(c) Symmetry Design Systems*';
ss{43} = '*      All Rights Reserved      *';
ss{44} = '*      UNPUBLISHED LICENSED SOFTWARE      *';
ss{45} = '*      Contains Proprietary Information *';
ss{46} = '*      Which is The Property of      *';
ss{47} = '*      SYMMETRY OR ITS LICENSORS      *';
ss{48} = '*Commercial Use or Resale Restricted *';
ss{49} = '*      by Symmetry License Agreement *';
ss{50} = '*****';
ss{51} = '* Model generated on Jul 31, 13';
ss{52} = '* MODEL FORMAT: SPICE3';
ss{53} = '* Symmetry POWER MOS Model (Version 1.0)';
ss{54} = '* External Node Designations';
ss{55} = '* Node 1 -> Drain';
ss{56} = '* Node 2 -> Gate';
ss{57} = '* Node 3 -> Source';
ss{58} = 'M1 9 7 8 8 MM L=100u W=100u';
ss{59} = '* Default values used in MM:';
ss{60} = '* The voltage-dependent capacitances are';
ss{61} = '* not included. Other default values are:';
ss{62} = '*      RS=0 RD=0 LD=0 CBD=0 CBS=0 CGBO=0';
ss{63} = '.MODEL MM NMOS LEVEL=1 IS=1e-32';
ss{64} = '+VTO=2.68841 LAMBDA=0 KP=76.5747';
ss{65} = '+CGSO=4.95684e-06 CGDO=1e-11';
ss{66} = 'RS 8 3 0.0207068';
ss{67} = 'D1 3 1 MD';
ss{68} = '.MODEL MD D IS=1.18893e-11 RS=0.0041311 N=1.07679 BV=68';
ss{69} = '+IBV=0.00025 EG=1 XTI=2.39558 TT=0';
ss{70} = '+CJO=1.95548e-09 VJ=0.708387 M=0.9 FC=0.5';
ss{71} = 'RDS 3 1 1e+09';
ss{72} = 'RD 9 1 0.0111061';
ss{73} = 'RG 2 7 12';
ss{74} = 'D2 4 5 MD1';
ss{75} = '* Default values used in MD1:';
ss{76} = '*      RS=0 EG=1.11 XTI=3.0 TT=0';
ss{77} = '*      BV=infinite IBV=1mA';
ss{78} = '.MODEL MD1 D IS=1e-32 N=50';
ss{79} = '+CJO=6.81119e-10 VJ=1.5551 M=0.9 FC=1e-08';
ss{80} = 'D3 0 5 MD2';
ss{81} = '* Default values used in MD2:';
ss{82} = '*      EG=1.11 XTI=3.0 TT=0 CJO=0';
ss{83} = '*      BV=infinite IBV=1mA';

```

```

ss{84} = '.MODEL MD2 D IS=1e-10 N=0.4 RS=3.00001e-06';
ss{85} = 'RL 5 10 1';
ss{86} = 'FI2 7 9 VFII2 -1';
ss{87} = 'VFII2 4 0 0';
ss{88} = 'EV16 10 0 9 7 1';
ss{89} = 'CAP 11 10 9.74541e-10';
ss{90} = 'FI1 7 9 VFII1 -1';
ss{91} = 'VFII1 11 6 0';
ss{92} = 'RCAP 6 10 1';
ss{93} = 'D4 0 6 MD3';
ss{94} = '* Default values used in MD3:';
ss{95} = '* EG=1.11 XTI=3.0 TT=0 CJO=0';
ss{96} = '* RS=0 BV=infinite IBV=1mA';
ss{97} = '.MODEL MD3 D IS=1e-10 N=0.4';
ss{98} = '.ENDS nvmfd5485nltlg';
ss{99} = '.control';
ss{100} = [' temperature = ' num2str(x(10))];
ss{101} = ' TRAN 0.001ms 7.5ms';
ss{102} = ' *plot mag(V(2))i(Vsys)';
ss{103} = ' write Active_Clamping.csv V(2) mag(i(Vsys))';
ss{104} = 'quit';
ss{105} = '.endc';
ss{106} = '.end';

```

```

%Save SPICE Script as a Circuit File in Matlab Working Directory
CircuitFileName = 'Active_Clamping.cir';
ckt_file = char(ss); %Conver cell array "ss" ti character Array
[rows,~] = size(ckt_file); %Read number of rows in "ckt_file".
fid = fopen(CircuitFileName,'w+');%File identified opened.
for i = 1:rows %Save each row of character array
    fprintf(fid, '%s',ckt_file(i,:));%"ckt_file" in ASCII file
    fprintf(fid, '%s\r\n', ''); %Circuit file name
end

```

```

fclose(fid); %File identifier closed.

```

```

%Run Winspice Circuit File

```

```

ExecFile= 'C:\WINSPICE\PF_ARC\wspice3 ';
system([ExecFile CircuitFileName]);

```

```

%Read WinspiceOutput Files

```

```

Active_C_file = csvread('Active_Clamping.csv',1,0); %Read transient responses
time = Active_C_file(:,1); %Creating time array
R = Active_C_file(:,2); %Creating Voltage magnitude array
Cur= Active_C_file(:,3); %Creating Current magnitude array

```

```

%Erase WinSpice Output Files

```

```

delete Active_Clamping.csv;

```

```

end

```

```

%José Antonio Rodríguez Castañeda   md193781
%Optimization-Based Modeling and Design of Electronic Circuits
%Usage: [time, R, Cur]=AC(x)
% X = [Vb R4 C1]', design variables.
% AVAC: Magnitud response of the Circuit.
% f: Frequency array with the corresponding Frequency points
function [time ,R,Cur] = AC(x)

%Optimization parameters & Preassigned parameters

Temp=25; %Temperature in °C
Vb=x(1); %Zener BreakDown Voltage
R1=100; %Resistor Values (Ohms)
R2=4700; %Resistor Values (Ohms)
R3=1000; %Resistor Values (Ohms)
R4=x(2); %Resistor Values (Ohms)
RL=6.8; %Resistor Values (Ohms)
C1=x(3); %Capacitor Value (nF).
C2=10; %Capacitor Value (nF).

if Temp==25 %Zener BreakDown Voltage
Vb=Vb;
elseif Temp==105
Vb=Vb+4; %105°C (0.05V/°C)
else
Vb=Vb-3.25; % -40°C (0.05V/°C)
end
LL=4.5; %Inductor Value (mH).

Ynom = [R1 R2 R3 R4 RL C1 C2 Vb LL Temp]; % Selected parameters vector.

[time ,R,Cur] = AC_SPICE(Ynom); %Execute Winspice driver

end

```

2.- Results of the third starting point

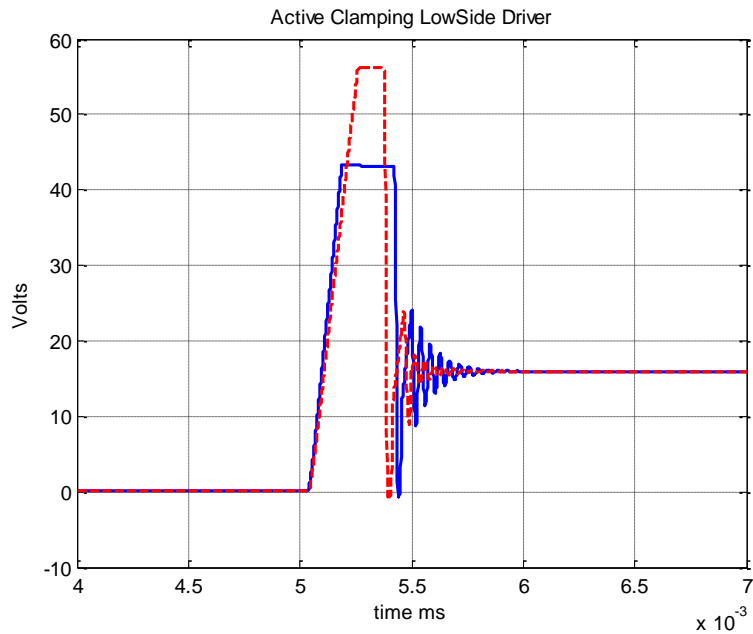


Figure 8.

*****Active Clamping ON Time and Power Optimization Algorithm *****

***** Starting point *****

x0 = 40 59 2

Power (mW) at initial Point
P = 7.853874144144006

On time (us) at initial Point
OT = 2.330000000000309e+002

Solution found
xp = 53.053658160427823 37.571466316942953 2.291184455003986

Power (mW) at solution
P = 3.423318359992859

On time (us) at solution
OT = 1.150000000000161e+002

Function Value at the solution
fval = 0.072866066975153

Number of iterations
ans = 45

Number of Function Evaluations

ans = 84

Exit Flag

EF = 1 fminsearch converged to a solution x.

D. REFERENCES

- [1] L. Guzzella and C. Onder, Introduction to Modeling and Control of Internal Combustion Engine Systems. Springer Science & Business Media, 2009.
- [2] S. Mallik, N. Ekere, C. Best, and R. Bhatti, “Investigation of Thermal Management Materials for Automotive Electronic Control Units,” Applied Thermal Engineering, vol. 31, no. 2–3, p. 355, Oct. 2010.
- [3] Widiastuti, Dian & Yansyah, Ferdi & Alaydrus, Mudrik. (2016). Bandstop Filter for Radar Application with L Resonator.